Journal of Science: Advanced Materials and Devices 1 (2016) 256–272

Contents lists available at ScienceDirect

Journal of Science: Advanced Materials and Devices

journal homepage: www.elsevier.com/locate/jsamd

Review Article

A review on organic spintronic materials and devices: II. Magnetoresistance in organic spin valves and spin organic light emitting diodes

Rugang Geng [a], Hoang Mai Luong [a], Timothy Tyler Daugherty [a], Lawrence Hornak [b], Tho Duc Nguyen [a, *]

[a] Department of Physics and Astronomy, The University of Georgia, Athens, GA 30602, USA
[b] College of Engineering, The University of Georgia, Athens, GA 30602, USA

ARTICLE INFO

Article history:
Received 15 August 2016
Accepted 20 August 2016
Available online 3 September 2016

Keywords:
Magnetoresistance
Organic spintronics
Spin transport
Spin diffusion length
Tunneling

ABSTRACT

In the preceding review paper, Paper I [Journal of Science: Advanced Materials and Devices 1 (2016) 128–140], we showed the major experimental and theoretical studies on the first organic spintronic subject, namely organic magnetoresistance (OMAR) in organic light emitting diodes (OLEDs). The topic has recently been of renewed interest as a result of a demonstration of the magneto-conductance (MC) that exceeds 1000% at room temperature using a certain type of organic compounds and device operating condition. In this report, we will review two additional organic spintronic devices, namely organic spin valves (OSVs) where only spin polarized holes exist to cause magnetoresistance (MR), and spin organic light emitting diodes (spin-OLEDs) where both spin polarized holes and electrons are injected into the organic emissive layer to form a magneto-electroluminescence (MEL) hysteretic loop. First, we outline the major advances in OSV studies for understanding the underlying physics of the spin transport mechanism in organic semiconductors (OSCs) and the spin injection/detection at the organic/ferromagnet interface (spinterface). We also highlight some of outstanding challenges in this promising research field. Second, the first successful demonstration of spin-OLEDs is reviewed. We also discuss challenges to achieve the high performance devices. Finally, we suggest an outlook on the future of organic spintronics by using organic single crystals and aligned polymers for the spin transport layer, and a self-assembled monolayer to achieve more controllability for the spinterface.

1. Introduction

Organic electronics has emerged as a vibrant field of research and development involving chemistry, physics, materials science, engineering, and technology. The material advantages include its rich physics, flexible chemistry, and cost efficiency. Organic semiconductors (OSCs) including π-conjugated polymers and small molecules promise the advent of mass production and fully flexible devices for large-area displays, solid-state lighting over a broad wavelength range, solar cells, and field effect transistors [1–3]. For the basic research, π-conjugated materials are fascinating systems in which a rich variety of new concepts have been uncovered due to the interplay between their π-electronic structure and their geometric structure. At first glance, charge transport in OSCs seems to be seriously suffered from its relatively low mobility caused by charge hopping/tunneling transport, a known characteristic for the electronic property in a disordered system. It is challenging to achieve a comprehensive understanding of the fundamental charge injection and transport in organic electronic devices. Nevertheless, from this complicated charge transport, the fascinating concept of organic magnetoresistance (OMAR) in organic light emitting diodes (OLEDs) was discovered. OMAR has recently has been found to be larger than 1000% at room temperature which is promising for magnetic sensor and lighting applications. It was shown by several groups that the larger OMAR effect is associated with the slower hopping transport or smaller hopping mobility. OSCs possess small intrinsic spin orbit coupling (SOC) and hyperfine interaction (HFI) due to their light-weight molecules constitution and the nature of π-orbital electron transport. Several different types of SOCs

* Corresponding author.
E-mail address: ngtho@uga.edu (T.D. Nguyen).
Peer review under responsibility of Vietnam National University, Hanoi.

http://dx.doi.org/10.1016/j.jsamd.2016.08.006

developed for crystalline semiconductors [4–8] may not be applicable to the organic materials used in organic spintronic devices. Due to relatively small spin-related interaction, the net effect from the spin scattering sources in the OSCs is very weak so that their spin relaxation time (in the μs range) is several orders of magnitude larger than in inorganics (in the ns range). This is an important ingredient for obtaining the high performance organic spin valves (OSVs) and Spin-OLEDs.

In the first part of this work (Paper I) [9], we presented a thorough review of the first organic spintronic phenomenon, OMAR in OLEDs where the slow charge hopping in the randomly oriented hyperfine field is believed to be the main ingredients for obtaining the effect. In this part, we concentrate on (i) magnetoresistance (MR) in OSVs, where spin injection/detection at the organic/ferromagnet interface and spin transport in OSCs are investigated, and (ii) spin-OLEDs or bipolar-OSVs where the spin-polarized electron and hole are injected from ferromagnetic (FM) electrodes causing the hysteretic loops of the device luminescence. Firstly, we will present the basic concepts used in OSVs. The major advances and challenges in OSVs will be highlighted. Secondly, the recent advances in fabricating spin-OLEDs and the challenges for getting the high performance of spin-OLEDs will be reviewed and analyzed. Finally, we suggest an outlook on the future of organic spintronics by using organic single crystals and aligned polymers.

2. Basic concepts

In this section, we will review the basic concepts on spin injection/detection and spin transport in the vertical spin valve structure where the polarized spin of holes is considered. Spin-electronics or spintronics employs spin degree of freedom of electrons in addition to their charge in solid state systems and manipulates it by an external force for the current information storage and future spin-based logic devices. A semiconductor-based spin valve consists of three important aspects for its successful operation: (i) injection of spins from a FM electrode into a semiconducting spacer, (ii) spin transport and manipulation in the spacer, and (iii) spin detection at another FM electrode. In general, there are various experimental techniques used to probe the polarized spin in these processes. First, depending upon the nature of the spin transport materials, different techniques have been used for the spin injections such as optical pumping by a circularly polarized light [10–11] or by two-photon photo emission [12,13], spin injection from FM electrodes by applied bias voltage [14,15] or by ferromagnetic resonance spin pumping [16,17], and by temperature gradient in the case of spin-Seebeck [18,19]. Second, the spin manipulation schemes in the spacer can be accomplished by magnetic field (Hanle effect) [20], electric field (Rashba effect and Stark effect) [21,22] and by various magnetic and spin resonances [23,24]. Finally, the spin detection schemes include detection of circularly polarized light [25], transient Kerr/Faraday linearly polarized light rotation [26,27], spin Hall voltage [28,29], electric resistance change [14,30], and tunneling-induced luminescence microscopy [31,32]. Among these techniques, electrical injection/detection has up until now been the most convenient method from the device perspective, especially in the organic spintronics. We note that the notion of strong SOC and well-defined band transport in organics are absent, the optical spin injection/detection in these materials is inhibited. In this review, we will focus on the spin injection/detection and transport of holes in OSVs through the electric method only.

To investigate spin transport using a vertical OSV architecture (Fig. 2a), a polymer/small molecule film is sandwiched between two FM electrodes with different coercive fields, B_c. We note that since most existing FM materials have high work functions (Table 1) close to the highest occupied molecular orbitals (HOMO) of the OSCs (Table 2), only holes are generally injected into and detected from the materials. Therefore, there is no light activity happening in the OSVs unless the effective work function of one electrode is engineered so that the spin polarized (SP) electrons can be injected into the emissive organic layer. Such bipolar OSVs or spin-OLEDs will be discussed in Section 4. Since $B_{c1} \neq B_{c2}$, it is possible to switch the relative magnetization directions of the FM electrodes between parallel and anti-parallel alignments, upon sweeping the external magnetic field, B (Fig. 2b). The device resistance at B, R(B), is then dependent on the relative magnetizations. The MR response is commonly defined as: MR = [R(B)-R(P)]/R(AP), where R(P)(R(AP)) is the device resistance for parallel (anti-parallel) magnetization configuration. Transport of SP carriers from the first FM electrode to the second depends upon the spacer properties such as spin scattering sources including HFI and SOC, and mobility which is affected by disorder, impurities, and temperature *etc.* of the materials [7,8,33,34]. In general, the spin polarization of the transport electrons in the OSCs is attenuated exponentially as e^{-d/λ_S} when electrons diffuse across the organic spacer with the thickness, d, λ_S is the spin diffusion length of the carriers in the organic spacer that depends on mobility, μ, and spin relaxation time, τ, of the transport electron following the relation:

$$\lambda_S = \sqrt{\mu k_B T \tau / e} \tag{1}$$

where k_B, T, and e are the Boltzmann constant, the material temperature, and the carrier charge, respectively [8,17,35–40]. In principle, the MR response of a device can be tuned by manipulating the spin relaxation time in its semiconducting spacer. However, the organic films are highly disordered and μ in these films is typically about five orders of magnitude smaller than that in inorganic semiconductors. Therefore, although τ in OSCs is long, the relatively low hopping mobility limits its spin diffusion length at lower than 100 nm in comparison to several micrometers in inorganic semiconductors [41,42]. The giant MR magnitude observed in OSVs can be adopted by modifying the Julliere's formula on the tunnel barrier of magnetic tunnel junction into the form [43]:

$$\frac{\Delta R}{R} = \frac{2P_1P_2e^{-d/\lambda_s}}{1 + P_1P_2e^{-d/\lambda_s}} \tag{2}$$

where P_1 and P_2 are effective carrier spin polarization injected from the magnetic electrodes. We note that the sign of the equation changes based on whether the R(AP) or R(P) is used as reference for the resistance change. Due to strong dependence of interfacial spin polarization, dubbed spinterface on the nature of the organic/metal contact, P_1 and P_2 might be very different from the spin polarization measured at the surface of the bulk FM materials [44,45]. The spinterface effect has recently attracted significant attention in

Table 1
Potential ferromagnetic materials for spintronic devices and their properties.

FM Electrode	Polarization P (%)	Work Function (eV)	Curie Temperature T_c (K)
LSMO	~100 [66]	4.8 [14]	360 [61]
Co	34 [67]	4.9 [14]	1388 [68]
Fe	44 [67]	4.5 [69]	1043 [70]
Ni	31 [71]	5.15 [69]	631 [70]
CrO_2	~100 [72]	3.4–6.9 [73]	390 [74]
$Fe_{50}Co_{50}$	50 [71]	4.7 [75]	720 [76]
Fe_3O_4	−80 [77]	5.5 [78]	860 [79]
$Ni_{81}Fe_{19}$	45 [71]	4.5 [75]	869 [80]
Co_2MnSi	~100 [81]	4.5 [82]	985 [83]

Table 2
Various organic spin valves combined with the properties of the ferromagnetic electrodes and organic semiconductors (OSCs).

OSCs	FM Electrodes	Carrier mobility ($cm^2 V^{-1} s^{-1}$)	Organic electronics and energy level	MR%@Temperature	Typical spin diffusion length
T_6	LSMO/LSMO [84]	$7.5*10^{-2}$ (p) [105]	Electron donor HOMO = −4.9 eV LUMO = −2.5 eV [106]	30%@RT [84]	70 nm; 10^{-6} s [84]
Alq_3	LSMO/Co [14] Fe/Co [49] Co/Al_2O_3/Py [91]	$2.5*10^{-5}$ (n) [107]	Light emitter HOMO = −5.7 eV LUMO = −2.8 eV [14]	−40% @11 K [14] 5%@11 K [49] 7.5%@4.2 K, 6%@RT [91]	45 nm@11 K [14]
α-NPD	LSMO/Co [94]	$6.1*10^{-4}$ (p) [108]	Hole transporting (OLEDs) HOMO = −5.4 eV LUMO = −2.4 eV [108]	14 ± 3% @14 K [94]	
RRP3HT	LSMO//Co [6] $Fe_{50}Co_{50}/Ni_{81}Fe_{19}$ [75]	$2.8*10^{-1}$ (p) [109]	Electron donor (OPV) HOMO = −5.1 eV LUMO = −3.5 eV [90]	80%@5 K, 1.5% @RT [6] 22%@5 K, 0.5%@RT [90]	62 ± 10 nm [75]
TPP	LSMO/Co [88]	$7*10^{-3}$ (p) [110]	Red emitter(OLEDs) HOMO = −4.9 eV LUMO = −3.1 eV [111]	17%@80 K [88]	
Rubrene	Fe/Co [41] /Fe_3O_4/Co [112]	40 (p) [113,114] $8*10^{-1}$ (n) [115]	OFETs, yellow dopant (OLEDs) HOMO = −5.4 eV LUMO = −3.2 eV [116]	16% @4.2 K, 6% @ RT [41] 6% @ RT [112]	13.3nm@0.45K [41]
Pentacene	LSMO/LSMO [117,118]	5.5 (p) [119] 2.7 (p) [120]	OFETs, Electron donor (OPV) HOMO = −4.9 eV LUMO = −3.0 eV [121]	6% @5.3 K [117] 2% @9 K [118]	
TPD	Co2MnSi/Co [122] LSMO/Co [122]	$1.2*10^{-3}$ (p) [123]	Hole transporting (OLEDs) HOMO = −5.4 eV LUMO = −2.5 eV [124]	7.8% @RT [122] 19% @5 K [122]	
CuPc	Fe/Co [125] LSMO/Co [126]	$1.5*10^{-1}$ (p) [127]	OFETs HOMO = −5.3 eV LUMO = −3.6 eV [128]	6.4% @40 K [125] −6% @10 K, −0.84% @RT [126]	60 nm @10 K [126]
CVB (BCzVBi)	LSMO/Co [94]	10^{-3} (p) [129]	Blue dopant (OLEDs) HOMO = −5.4 eV LUMO = −2.5 eV [130]	(R)18 ± 3% @14 K [94]	
P(NDI2OD-T2)	LSMO/Co [131]	$6*10^{-2}$ (n) [132]	OFETs HOMO = −5.6 eV LUMO = −4.0 eV [131]	90% @4.2 K 6.8% @ RT [131]	64 nm @4.2 K [131]
BCP	Co/NiFe [133]	$1.1*10^{-3}$ (n) [134]	Electron transporting (OLEDs) HOMO = −6.5 eV LUMO = −3.5 eV [133]	3.5% @RT [133]	

organic spintronics due to the complication of orbital-hybridization at the interface between organics and FM electrodes. This topic will be discussed in Section 3.

Now, we would like to review the general challenges encountered and solutions achieved for spin injection/detection in semiconducting spin valves. Because the carrier density with spin-up and spin-down are equal in the semiconductor spacer, no spin polarization exists in it if the material is in thermal equilibrium. Therefore, in order to achieve SP carriers, the semiconductor needs to be driven far out of equilibrium and into a situation characterized by different quasi-Fermi levels for spin-up and spin-down charge carriers. Several calculations of spin injection from the FM metal into the inorganic semiconductor showed that a large difference in conductivity of the two materials inhibits a creation of an imbalance which creates difficulty in the efficient spin injection from metallic FM into semiconductors; this has been known in the literature as the "conductivity mismatch" hurdle [46–48]. There are three possible technical methods commonly used in inorganic spin valves to overcome the conductivity mismatch problem. (i) First, a tunnel barrier layer inserted between the FM metal and the semiconductor may effectively achieve significant spin injection [49]. In this case, the special extensions of charge wave functions for spin-up and spin-down electrons at the Fermi energy in FM materials are different; and this difference contributes to their spin injection capability through a tunneling barrier layer. Therefore, the tunneling barrier acts as a spin filter [50,51]. Control of the tunneling thickness and hence resistance of the insulating layer allows optimization of the spin injection capability. In general, the tunnel barrier could be introduced at the metal/semiconductor interface in two ways: tailoring the band bending in the semiconductor, which typically leads to Schottky barrier formation [52,53] or physically inserting a discrete insulating layer [20,54]. Interestingly, the conductivity mismatch has been thought to be less severe when using OSC since carriers are injected into the OSC mainly by tunneling through an insulating barrier naturally formed during the fabrication process [34,44,50,55–57]. For examples, several incredibly large MR responses in OSVs have been reported in the literature where the tunnel barrier was not explicitly used [36,44]. However, such a natural tunneling barrier is more likely to create challenges in controlling and optimizing the effective spin injection/detection in OSVs and in providing the reproducibility of the MR magnitude and even the sign of the MR response [14,44]. (ii) The second method for overcoming the conductivity mismatch problem is to use FM electrodes with a nearly 100% of spin polarization. For this reason, half-metals such as LSMO and CrO_2 which possess nearly perfect polarization at cryogenic temperature might be ideally used in OSVs [14,58,59]. It is worth noting that the spin polarization of these materials are very sensitive to the seed substrate and defect states such as impurities, crystallographic disorder, vacancies generated by the imperfect epitaxial growth [60]. In addition, the relaxation at the surface of the materials might substantially make the interfacial spin polarization different from the bulk magnetization [61]. So far, only LSMO has been extensively used in OSVs. The reason is that LSMO is quite robust against thermal, mechanical and chemical reactions; therefore multiple activities such as chemical and mechanical effects during cleaning process and high temperature spin transport spacer depositions, can be done on the films without substantial change in their

magnetic properties [14]. These superior properties make LSMO one of the best candidates for use as the bottom electrode in OSVs. (iii) Finally, the use of organic semiconducting FM electrodes with low conductivity can also be a possible solution for overcoming the conductivity mismatch problem [62–65]. Some popular metals/half-metals as FM electrodes in spin valves and their spin polarization, work function, and Curie temperature collected from different references are listed in Table 1.

3. Organic spin valves

The first organic spintronic sandwiched device, LSMO($La_{2/3}Sr_{1/3}MnO_3$)/T_6/LSMO with a lateral structure was designed and tested by Dediu et al., in 2002 [84]. They observed a large change in resistance of the structure at room temperature due to an applied magnetic field that suggested the successful spin injection into T_6 (see Fig. 1) OSCs. In 2004, Xiong et al. [14] demonstrated the first vertical inorganic-organic hybrid spin valve device using organic molecule tris(8-hydroxyquinolinato) aluminium (Alq_3) as the non-metallic spacer sandwiched between LSMO and Co electrodes, similar to the one shown in the schematics of Fig. 2a. Several excellent review papers on OSVs can be seen in the literature [8,33,59,85,86]. Fig. 2b shows the magnetic hysteretic loop of the electrodes with coercive fields $H_c = 30$ Oe and 150 Oe for LSMO and Co, respectively. In a device of spacer thickness 130 nm, they recorded an MR of 40% at 11 K with a clear switching between the low and high resistances which corresponds to the magnetization switching between two electrodes (Fig. 2c). However, the measured device resistance had a lower value at anti-parallel magnetization – an unusual feature, which they attributed to the negative polarization of Co electrode, probably due to the domination of minority-spin injection in the Co d-band [14]. Later, several other research groups also observed the inverted MR effect in the Alq_3-based OSVs [59,87–90]. The inverse spin valve effect has been regularly observed in OSVs with thick Alq_3 spacer of about 100 nm range [34,59,87,89,90]. However, when the spacer is small of about 10 nm range, the positive MR has been found [44,91]. Santos et al. and Barraud et al. measured a positive tunneling magnetoresistance (TMR) using Co/Alq_3(1–4 nm)/NiFe and LSMO/Alq_3 (a few nanometers)/Co, respectively [44,91]. Nevertheless, the origin of this inverse MR effect is still not clear. This will be discussed in more detail later in this section.

The MR value in OSV depends strongly on the bias voltage [6,14,36,87]. Studies have shown that the MR decreases monotonically with the bias voltage and has an asymmetric behavior with the polarity of the voltage [6,14,36,92]. A representative of the bias voltage dependence of MR is shown in Fig. 2d. It is important to note that a similar observation was previously observed in a magnetic tunnel junction (MTJ) device using LSMO and Co [93]. This asymmetry may originate from injecting/detecting the SP carriers from the FM electrodes of different work functions. Here, the MR magnitude decreases less for negative bias voltage, at which the electrons were injected from LSMO. Different explanations of the bias voltage dependence of the MR have been put forward [94–96]. First, the applied voltage shifts the band of the electrode into which electrons tunnel downward, i.e. towards higher density of states. This alone decreases the MR magnitude with increasing bias. Next, an alternative mechanism is scattering of the injected electron spins from magnons generated from defect states at the interface such as magnetic impurities when it tunnels to the organic spacer. This scattering is suggested to be more effective at high applied voltage causing larger SP loss at high applied voltage [36,97].

After the early demonstrations of the MR effect on the hybrid OSVs, numerous studies have been performed on MR/TMR effect using a variety of π-conjugated small molecules and polymers [14,18,59,91,98–104]. The chemical structures of some of these molecules and polymers are shown in Fig. 1 while a summary of their electronic properties and the performance of OSVs using them as the spacers in between various FM electrodes as collected from various references are given Table 2. The studies on the OSVs have been directed into the following major categories: (i) seeking the evidence of the spin injection into and transport in OSCs, (ii) underlying mechanism for the spin loss in OSCs, and (iii) enhancement of the MR effect with high temperature operation.

3.1. Spin tunneling versus spin injection

The distinction between spin tunneling and spin injection in OSVs is challenging since the MR response in these phenomena essentially looks the same. In addition, both phenomena have similar MR dependence on the spacer thickness. Therefore, it was reasonable to raise a question regarding the spin injection in OSVs. For instance, the reports from Jiang et al. [135] claiming the absence of spin transport in Fe/Alq_3/Co OSV and Xu et al. [88] asserting no correlation between the MR and the thickness of the organic spacer

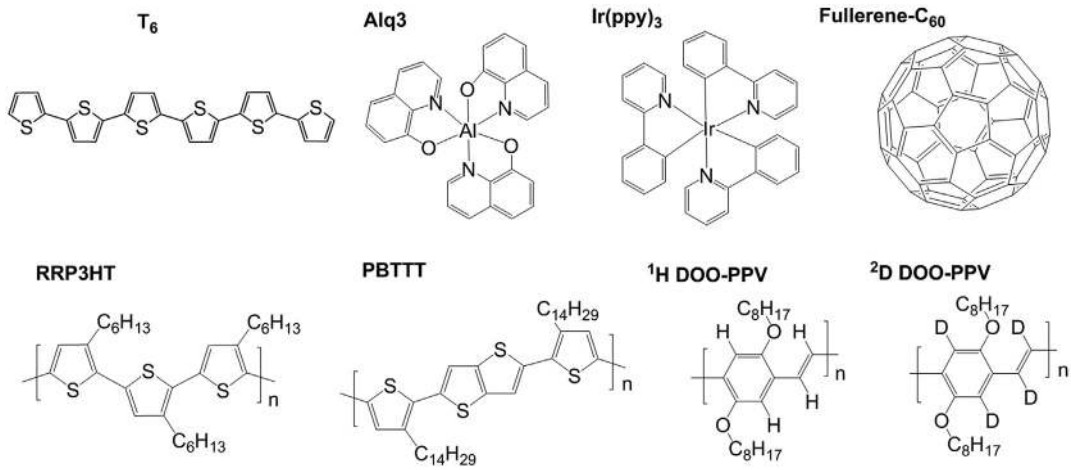

Fig. 1. Chemical structure of some organic semiconductors including small molecules and π-conjugated polymers: sexithienyl (T_6), tris(8-hydroxyquinolinato)aluminium (Alq_3), tris[2-phenylpyridinato-C2,N]iridium(III) ($Ir(ppy)_3$), fullerene-C_{60}, regioregular poly(3-hexylthiophene-2,5-diyl) (RRP3HT), poly[2,5-bis(3-tetradecylthiophen-2-yl)thieno[3,2-b]thiophene] (PBTTT-C14), protonated poly(dioctyloxy)phenylenevinylene (H-DOOPPV), and deuterated poly(dioctyloxy)phenylenevinylene(D-DOOPPV).

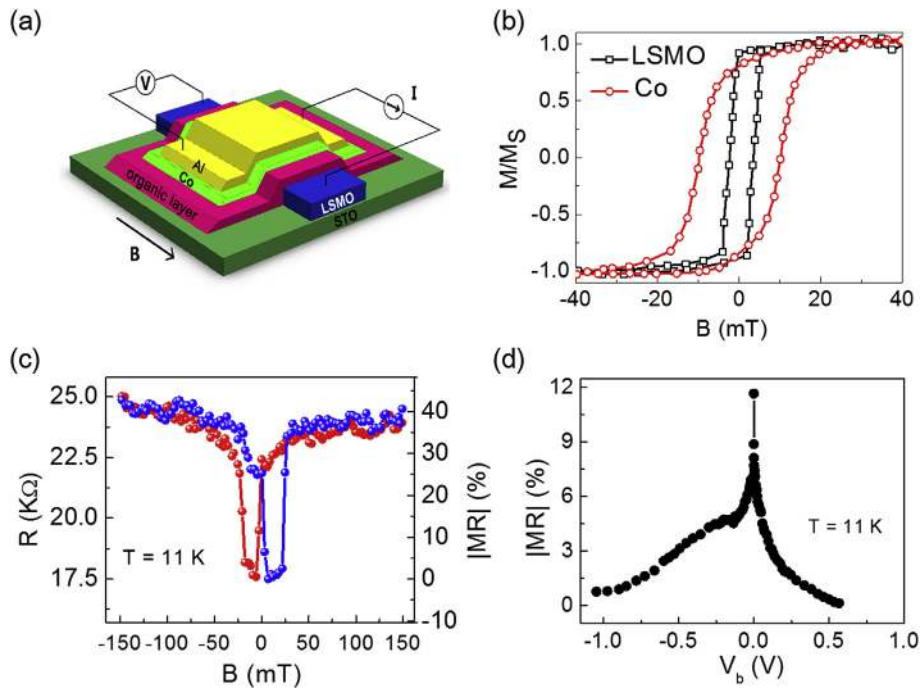

Fig. 2. Schematics of the organic spin valve (OSV) and its performance. (a) Schematic diagram of the OSV device. (b) The magnetization Kerr loops of the ferromagnetic electrodes. (c) The MR loops of the OSV measured at low temperature. (d) MR with bias voltage dependence at low temperature. Reproduced with permission [14].

questioned the spin diffusion through the OSCs affirmed previously. Jiang et al. also reported a similar MR effect to all measurable OSVs regardless of the spacer material, either (tetraphenyl porphyrin (TPP) or Alq_3. Similarly, Grünewald et al. [99] observed a similar spin valve effect in the device with only one FM electrode where the FM electrode for the spin detection is absent. These observations created the impression of the injection of the SP carriers into the OSCs from FM electrodes. There are several outstanding demonstrations of spin injection into organics from FM electrodes as listed in the following discussion:

(i) **Two-photon photoemission technique:** Cinchetti et al. [12] came up with a microscopic technique, namely "two-photon photoemission". They successfully demonstrated the injection of the SP carriers into OSCs. "two-photon photoemission" technique was employed to inject the SP carriers into a Co/CuPc heterojunctions and showed a spin injection efficiency of 85–90% at room temperature. In this technique, two successive laser pulses are sent on the metal-OSC heterojunction. The first pulse generates the SP electrons on Co film while the second pulse excites the SP electrons diffused into the OSC film from the FM electrode and then the OSC photoemits, hence giving rise to information about the spin injection into OSC layer from the electrode.

(ii) **Low-energy muon spin rotation:** Simultaneously, Drew et al. [19] showed the successful injection of the SP carriers into Alq_3 spacer and their transport by low energy muon spin rotation (LE-μSR) method in operational NiFe/LiF/Alq_3/TPD/FeCo devices. In this technique, the muons with 100% spin polarization are implanted from one electrode into the Alq_3 spacer where they lose energy very quickly and stop at a certain penetration depth depending on their muon implantation energy. The muon spin precesses around the local magnetic field for about 2.2 μs before decaying into two neutrinos and a positron, of which emission direction is correlated with the muon's spin direction at the time of decay. Therefore, the local magnetic field generated by the electron spin accumulation at a certain location in the organic spacer and hence the spin diffusion length can be extracted. They observed a dependence of the spin diffusion length on temperature, which was qualitatively in agreement with the temperature dependence of $-1/\ln(MR)$ in the devices (Fig. 3a).

(iii) **Isotope effect on spin transport:** The other way to show experimental evidence for the spin injection and spin transport in OSCs is to study the isotope effect on spin response of the OSVs based on DOO-PPV polymer (Fig. 1) [36]. The DOO-PPV materials were prepared by replacing all strongly coupled hydrogen atoms (^1H, nuclear spin $I = ½$) in the organic π-conjugated polymer poly(dioctyloxy) phenyl vinylene (DOO-PPV) spacer, with deuterium atoms (^2H, $I = 1$) having much smaller hyperfine coupling constant a_{HFI}, namely $a_{HFI}(D) = a_{HFI}(H)/6.5$. Therefore, the HFI strength in deuterated DOO-PPV is about 3 times weaker than that in hydrogenated DOO-PPV. The thickness dependent MR measured in these OSVs and their fits are shown in Fig. 3b. The result showed that the spin diffusion length in deuterated DOO-PPV is about three times longer compared to that in hydrogenated DOO-PPV. This is a solid evidence for the spin transport in OSCs.

(iv) **Ferromagnetic resonance spin pumping:** Recently, Ando et al. came up with a different technique, namely "ferromagnetic resonance (FMR) spin pumping", to inject SP carriers into the OSCs from FM electrode [16,17,136–138]. The technique has been well-established for injecting the spin from FM electrode into metals and inorganic semiconductors. Under either cw (continuous wave) or pulsed microwave excitation at its magnetic resonance, an exciting magnetization precession or spin wave is generated in the FM material [18,136]. Due to the strong spin-exchange coupling at the interface between FM and organics, these waves travel through the interface creating a spin current

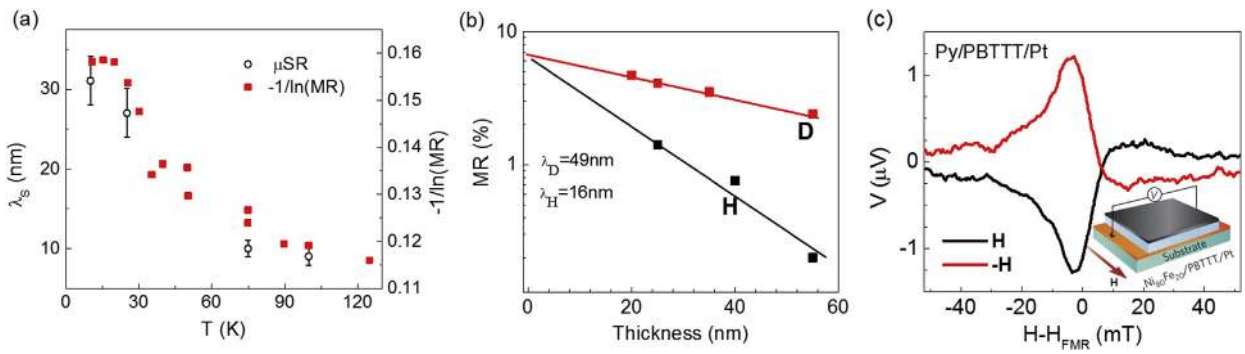

Fig. 3. Spin injection and transport through organic interlayers. (a) The temperature dependence of the spin diffusion length extracted from the muon measurements and its correlation with the temperature dependence of MR. Reproduced with permission [19]. (b) Thickness dependence of MR for two isotopes of one π-conjugated polymer. Reproduced with permission [36]. (c) Ferromagnetic resonance (FMR)-based spin current transport together with the electromotive force V measurement. The inset shows the schematic of the Py/PBTTT/Pt trilayer device. Reproduced with permission [17].

into the OSC interlayer. The spin current then generates an electric field, E based on the inverse spin Hall effect (ISHE) mechanism where the presence of SOC in the spin transport materials is a must. This technique does not require an applied bias voltage and therefore can avoid spurious effects such as anisotropic magnetoresistance and can be used to inject the spins without any conductivity mismatch problem.

(v) **IV characteristic of charge tunneling effect:** Another indirect technique is to study the IV characteristics of the devices while varying the spacer thickness [100,139,140]. In some cases, an insulator such as Al-oxide was used to avoid the short circuit and enhance the quality of the organic layer at its interface. The charge motion in the device obeys one step tunneling or multiple step tunneling (spin transport) [101,102]. The studied spacer thickness is normally less than 10 nm. The criteria taken from magnetic tunnel junctions for distinguishing charge direct tunneling and transport are the weak temperature dependence and the parabolic behavior of the IV characteristics [141]. However, the similar IV characteristics can also be observed in multiple step charge tunneling (charge/spin transport) normally happening in OSCs [101].

3.2. Spin diffusion length in OSCs

In the previous section, we showed various experimental evidence for the spin injection from FM electrodes to OSCs. Therefore, it is sufficient to talk about spin diffusion length in OSVs when the well-defined film thickness is far from the tunneling regime (normally larger than 10 nm). There exist several empirical techniques for extracting the spin diffusion length in OSCs:

(i) Firstly, the most popular technique is to measure the thickness dependent MR and fit them to the modified Jullière Equation (2). This method can give a reasonable value under the assumption that the injected spin polarization and the spin diffusion length remain the same when varying the thickness of the device. In addition, it is hard to precisely measure the thickness of the organic film due to the incontrollable metal inclusion during the top electrode fabrication. Therefore, the method has unavoidable uncertainty. Fig. 4 shows the MR values (normalized to their maximum) measured as a function of the interlayer thickness and their modified-Jullière fit for representative OSCs as extracted from different studies [14,75,131,141,142,155]. The figure depicts a general trend that the MR decreases significantly with the thickness and vanishes at a certain value. Both the thickest/thinnest limiting values were, however, material dependent. For instance, Xiong et al. [14] observed an ill-defined layer up to 100 nm Alq_3 spacer thickness based on the observation of linear I–V curve. For d > 100 nm, they observed a considerable decrease in the MR values with the thickness but still measurable up to d = 250 nm. From the fit to the modified Jullière formula, they obtained $P_1P_2 \sim -0.32$; $d_0 = 87$ nm; and $\lambda_s \sim 45$ nm. The product P_1P_2 obtained from the fit is consistent with the product of the polarization of LSMO and Co. Rybicki et al. [141] fabricated an OSV using the same molecule, Alq_3, and characterized it as a function of spacer thickness. Interestingly, they found that the spin diffusion length in Alq_3 is very sensitive with trap density intentionally generated by X-ray illumination from the E-beam source during the metal evaporation. The pristine Alq_3 shows 40 nm spin diffusion length while only 7 nm length was found in the X-ray illuminated films.

(ii) Secondly, Majumdar et al. [143] recently extracted the spin polarization of LSMO from the study of anisotropic magnetoresistance. This method allows them to calculate the spin diffusion length directly from the modified Jullière formula. Although the method can avoid the complication of studying thickness dependent MR, theirs method for extracting the spin polarization does not take into account the spinterface effect which is known to be serious in OSVs.

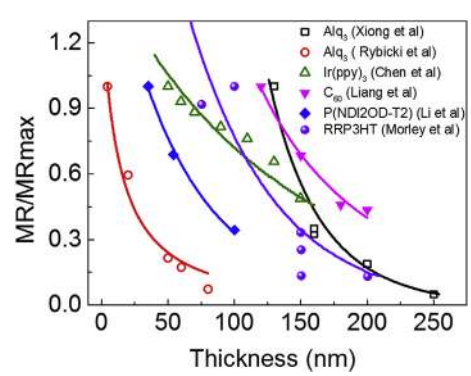

Fig. 4. Thickness dependence of the normalized MR in OSVs with various OSC interlayers measured by different groups (Xiong et al. [14]; Rybicki et al. [141]; Chen et al. [142]; Liang et al. [155]; Li et al. [131]; Morley et al. [75]).

(iii) Thirdly, of course, the most powerful method is to use the low-energy muon spin rotation done by Drew et al. but this is not a tabletop method that can be easily operated in the standard setup. Using this technique, the local magnetic field generated by the electron spin accumulation at the certain location in the organic spacer can be obtained for extracting the spin diffusion length. They found that the spin diffusion length of Alq_3 is about 30 nm at 10 K and about 10 nm at 90 K (Fig. 3a).

(iv) Fourthly, it is worth mentioning the study from Cinchetti et al. using the two photon photoemission technique [12]. The spin diffusion length of CuPC was estimated to be about 1 nm which is too small compared to the length of ~50 nm measured by the thickness dependent MR [126].

(v) Finally, from the induced voltage signal in the counter electrode and the induced pure spin current in OSCs in the FMR spin pumping experiments, the spin diffusion length of different polymers and small molecules has been extracted by a several groups [17,137,138]. In general, the spin diffusion length was found to be independent on the temperature [17,137]. In particular, the spin diffusion length in PBTTT polymers [17] is about 200 nm, in Alq_3 small molecules [137] is about 50 nm and in HDOO-PPV polymers [138] is about 25 nm. The discrepancy among the reported values of the spin diffusion length in the conventional polymers such as PBTTT and HDOO-PPV, raises a technical question on either the experimental reproducibility of the result or the models used.

In the above techniques, the minimization of the metal inclusion into the organic layers is necessary for the reproducibility of the result. Several advanced methods have recently been introduced for fabricating the top FM electrodes. Chen et al. showed the deposition of an FM electrode using the back scattering method avoiding the direct hit of the metallic atoms onto the organic films [144]. This method was reported to enhance the MR and was shown to be promising for the reproducibility of the OSV performance although unintentional impurities might be introduced during the slow metal evaporation at low chamber pressure (10^{-3} torr). In addition, Sun et al. used a buffer-layer assisted growth method (BLAG) where they first deposited several monolayers of high-density Co nanodots onto organic films at low temperature, followed by normal Co evaporation onto the OSC layer [92]. With this technique, the diffusion of Co onto the OSC spacer is highly suppressed yielding a large MR value (~300%) at 10 K.

3.3. Spin loss mechanism in OSCs

In the previous sections, strong evidence for spin injection and transport occurring in OSCs was presented. The spin diffusion length in organics is limited to less than 200 nm. So far the underlying mechanism for the spin loss mechanism in OSVs is still a hot debate. In general, it appears to be driven by SOC and/or HFI during the charge hopping transport. In this section, we will review several studies for the existence of either SOC or HFI as a dominant spin loss mechanism:

3.3.1. Hyperfine interaction domination

HFI has been experimentally proven to play an important role in spin transport in conventional polymer-based OSVs [36]. Nguyen et al. [36] demonstrated that the spin diffusion length in the DOO-PPV based OSVs is significantly enhanced when the hydrogen atoms at the chemical back bond are chemically substituted by deuterium atoms with much weaker HFI strength. The important role of HFI in the spin response in OLEDs and OSVs was also confirmed by a study of the ^{13}C-rich DOO-PPV polymers where spin-less ^{12}C atoms in the chemical backbone of the polymers were substituted by ^{13}C atoms causing stronger HFI than that in the hydrogenated DOO-PPV polymers [145,146]. The relatively weak SOC in DOO-PPV polymers recently reported by Sun et al. [138] In this report, the spin Hall angle, a measure of SOC strength in DOO-PPV was found to be several orders of magnitude smaller than those of the Pt-containing polymers and C60 fullerene. The result is in agreement with the general notion that SOC in conventional polymers and small molecules is relatively weak. We note that the study of HFI in OLEDs has significantly been achieved during the past decade. Nguyen et al. [147] reported no significant OMAR effect in C60 based diodes. However, when a side chain is introduced to a C60 molecule as in the case of C60 PCBM, measurable OMAR effect was observed [148]. They conjectured that the HFI introduced by the side chain causes OMAR effect. Another convincing piece of evidence of the role of HFI in observing OMAR in OLEDs is the study of isotope dependent OMAR where the width of the OMAR can be reliably controlled by the types of hydrogen or carbon isotopes in the molecules [146]. The role of HFI in OMAR response was comprehensively discussed in the first part of this review series.

3.3.2. Spin orbit coupling domination

Perhaps, the most convincing evidence for the existing of the intrinsic SOC in OSCs is the detection of the Hall voltage generated by the pure spin current in OSCs which is pumped from a FM electrode using the method named ferromagnetic resonance spin pumping [16,17,136,138]. Ando et al. first reported that both conducting and semiconducting polymers shows measurable SOC strength [17,136]. The spin diffusion length extracted from the spin current was estimated to be about 200 nm, much larger than the spin diffusion length reported by the other techniques (Fig. 3c) [17,136]. This raises a question why the spin diffusion length studied in similar systems, but different methods is much different. Koopmans commented that the large spin diffusion length found by Watanabe et al. might be because the HFI in the studied polymer is quenched by the considerably larger applied magnetic field of a few hundreds of mT during the magnetic resonance spin pumping [149]. A recent study of Sun et al. [138] using the method but with a pulsed microwave source shows that when the heavy Pt metal is included in polymers, much higher spin Hall angle than conventional polymer such as DOO-PPV was observed. This confirms that heavy metals introduce large intrinsic SOC for triplet exciton transition symmetry breaking found in various emissive organometallic molecules [150]. Beside this unique direct probe of OSC existence, Drew et al., on the other hand, found that the SOC plays an important role due to the lack of magneto-conductivity responses in OLEDs made of Alq_3 isotopes [40,151]. It is worth noting that by using the same method Sheng et al. previously demonstrated that the magneto-conductivity in Ir(ppy)3-based and Pt(ppy)3-based OLEDs has much broader response line width than that of Alq_3 [148,152]. The similar result was also obtained by Shakya et al. on the group III hydroxyquinolates [153]. This indicates that the SOC strength in the organometallic small molecules strongly increases with the heavy metal substitution. Therefore, there is no doubt that considerable SOC strength would exist in Alq_3 molecules. Nuccio et al. [154] suggested that even oxygen or sulfur atoms might be a great source for SOC.

So far, only the intrinsic SOC has been discussed. As mentioned above, there might exist other types of SOCs that are associated with the crystallinity of the materials. Recently, Liang et al. investigated another type of SOC namely curvature-enhanced SOC in the buckyball C60 and C70 molecules by two complementary spin-dependent techniques namely OMAR in OLEDs and MR in OSVs.

The curved structures of C60 and C70 molecules are well-defined and slightly different. Since naturally abundant ^{12}C has spinless nucleus, the HFI in these two materials is treated to be negligible. However, they both have the same intrinsic SOC. Fig. 5a shows the spin diffusion length measured by thickness dependent MR of those materials at 120 K. The spin diffusion length in C70 is estimated to be about 123 nm, clearly longer than about the length of 86 nm in C60. Liang et al. found that this tendency remained the same at all temperatures. The stronger SOC in C60 was confirmed by the OMAR study where the width of OMAR in C60 is 26 mT, larger than the width of 20 mT in C70 (Fig. 5b). The result was later confirmed by Sun et al. [138] who showed significantly large spin Hall angle in C60 film compared to the angles in several conventional polymers where only intrinsic SOC exists (Fig. 5c). This is a strong evidence that the strong SOC found in fullerene is mainly caused by the curvature-enhanced SOC. Since such SOC is strongly dependent on the interfaces, the polycrystalline degree of the film is a very important factor for determining the SOC strength in the film. In fact, the report of spin diffusion length from group varies significantly, probably due to differences in film morphology [138,155–159].

It is worth noting that in addition to this evidence of the existence of the HFI and SOC, there are several demonstrations that both mechanisms do not work in OSVs. For example, the measured spin diffusion length in $Ir(ppy)_3$, one of the most popular and strongest phosphorescent materials used in OLEDs, is comparable with that in Alq_3 with much smaller SOC [126]. This implies that either the tunneling might happen in the device or a special spin transport mechanism such as the spin exchange coupling happens in OSVs [160].

In addition to experiments designed to probe the SOC and HFI in OSCs, several theoretical papers have been proposed. Bobbert et al. [37] proposed a HFI-based theory for spin diffusion in disordered OSCs based on incoherent hopping of a charge carrier and coherent spin precession under the effect of local magnetic field comprised of a random nuclear field and applied magnetic field. The different HFI fields at different hopping sites also give rise to spin relaxation. They found that the diffusion length is strongly dependent on the dwell-time for the carrier at a certain hopping site compared to the hoping time between two sites. Yu proposed a SOC-based theory of carrier spin relaxation in which the spin diffusion length depends on the mean charge hopping distance and the SOC strength [38]. He found that the spin diffusion length monotonically decreases with an increase in temperature and then gets saturated when the charge hopping length is equal to the nearest neighbor distance. Based on these two theoretical papers, the HFI only affect the spin dynamics when it is located at a certain sites while SOC affects the spin dynamics during the hopping time between two sites. Interested readers might refer to other interesting papers [39,161,162].

3.4. Room temperature magnetoresistance

One of the important goals of OSVs is to obtain large MR at room temperature. Perhaps, vanishing MR at room temperature is one of the serious obstacles for realizing practical applications of OSVs. In the first report by Xiong et al. [14], 40% MR was reported at 11 K but decreased steeply with increasing T and vanished at room temperature (Fig. 6b). Based on the modified Jullière equation, one can expect two scenarios in which effective injection of spin polarization or/and spin diffusion length are quenched at high temperature.

(i) For the former, Xiong et al. originally attributed the MR reduction to the reduction of spin diffusion length since the temperature dependence of the magnetization of LSMO measured by magneto-optical Kerr effect (MOKE) (Fig. 6a) is much weaker than that of the MR reduction (Fig. 6b) while the magnetization of Co is almost a constant. However, the magnetization measured by MOKE might not reflect the truly interfacial spin polarization of LSMO since the penetration depth of the probe light in LSMO is on the order of 10 nm where spin injection happens in a few nanometers from the interface. Instead, Park et al. [61] demonstrated a much stronger temperature dependence of the surface magnetization of LSMO (measured by spin-resolved photoemission spectroscopy (SPES)) compared to its bulk magnetization (measured by superconducting quantum interference device (SQUID)). Fig. 6a clearly shows that the magnetization and hence the spin polarization at the surface decreases much faster with temperature and vanishes at Curie temperature T_c. The trend of the temperature dependence of the surface polarization is more likely to be responsible for the temperature dependent MR measured by Xiong et al. and other groups as described in Fig. 6b [14,90,94,159,163]. Although it is reasonable to assign the reduction of MR with temperature to the LSMO interfacial spin polarization reduction, the above study does not account for the spinterface effect at LSMO and Co electrodes. The surface spin polarization of those materials might be very different with the presence of other molecules at the interface. In fact, the MR quenches even faster with temperature in several studies when other FM materials such as Fe, NiFe and FeCo with relatively large Tc were used (see Tables 1 and 2) [19,49,75,133]. This strongly suggests that the spinterface at top FM electrode used in the studies in Fig. 6b must be investigated for the MR quenching

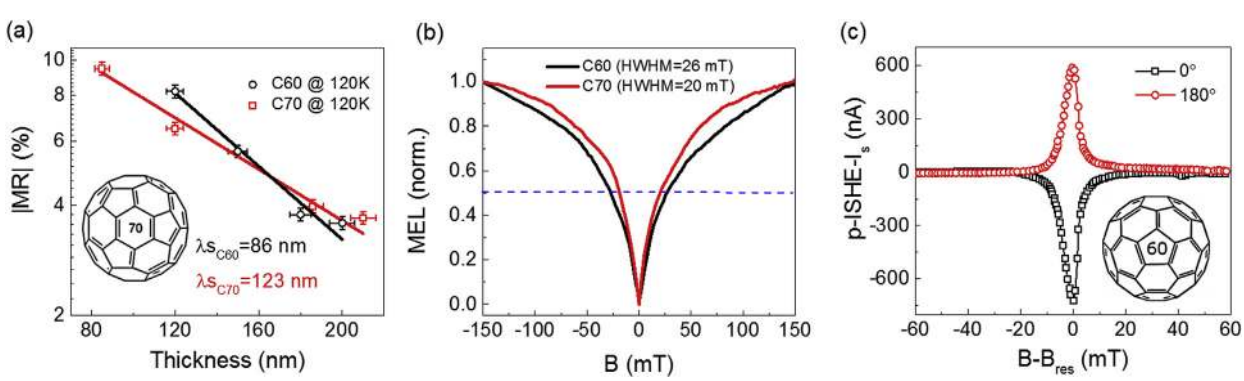

Fig. 5. Various magnetic field effects in fullerene-based OSC devices. (a) Thickness dependence of MR in fullerene-based OSVs. Reproduced with permission [155]. (b) Magneto-electroluminescence (MEL) in fullerene-based OLEDs. Reproduced with permission [155]. (c) Pulse-inverse spin Hall effect (p-ISHE) response in fullerene-based trilayer device. Reproduced with permission [138].

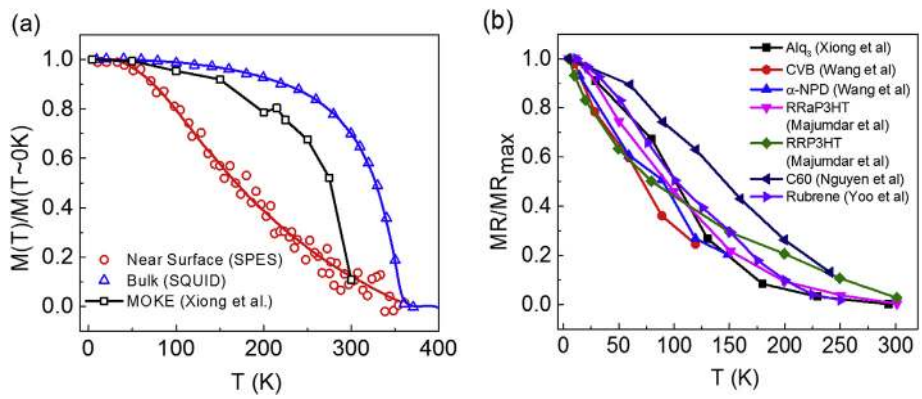

Fig. 6. (a) Temperature dependent magnetization of LSMO measured by AQUID and SPES techniques (Park et al. [61]), and by MOKE (Xiong et al. [14]) (b) Temperature dependence of normalized MR in OSVs with various OSC interlayers measured by different groups (Xiong et al. [14]; Wang et al. [94]; Majumdar et al. [90]; Nguyen et al. [159]; Yoo et al. [163]).

at high temperature. We note that Liang et al. [155] and Li et al. [131] recently reported the relative insensitivity of the spin diffusion length to temperature in fullerene and conjugated polymer, respectively.

(ii) For the latter, some studies [6,164] demonstrated that the spin diffusion length of the OSCs decreases with increasing temperature. This explanation was supported by a direct measurement of spin diffusion length of Alq_3 using LE-μSR and its correlation with temperature dependent MR as performed by Drew et al. [19] (Fig. 3a). However, their result seems to contradict the spin diffusion length result reported from the magnetic resonance spin pumping where the spin diffusion length in Alq_3 is independent on the temperature [137].

The other way to evaluate the temperature dependence of MR is to estimate the charge mobility and spin relaxation time versus temperature. For example, the electron spin-lattice relaxation rate in Alq_3 measured by the spin-1/2 photoluminescence detected magnetic resonance was found to be temperature independent [94]. Since the mobility of Alq_3 increases with increasing temperature, one can estimate from Equation (1) that the spin diffusion length in Alq_3 should increase with the temperature. This conflicts with the result reported by Jiang et al. as well as by Drew et al. for the same material [19,137]. This raises the question of the validity of equation (1) in organics or whether the spin-lattice relaxation time measured by magnetic resonance in general can be used to estimate the spin diffusion length of moving charge under applied electric field. This open question is related to the nature of the spin transport in OSCs which is still under debate [165].

It is important to note that a large volume of studies can be found in the literature in support of the first scenario. Nevertheless, the above discussion suggests that obtaining large MR at higher temperature requires the use of FM electrodes with high polarization and high T_c and the OSCs with long spin diffusion length at higher temperature. Despite the mechanism causing MR quenching at high temperature, some recent studies have been encouraging towards obtaining the larger MR effect at room temperature [6,91,122,131,158]. So far, the MR of nearly 10% at room temperature has been reported in both small molecule- and polymer-based OSVs. The first room temperature MR of about 1.5% on the LSMO/region-regular P3HT(100 nm)/Co OSVs with 100 nm was observed by Majumdar et al. [6] by annealing the organic film before the top electrode evaporation. In 2007, Santos et al. showed a TMR ~5% at room temperature in $Co/Al_2O_3/Alq_3$(<2 nm)/NiFe magnetic tunnel junction [91]. The inclusion of Al_2O_3 in between the Co and Alq_3 layer makes the device different from the previously studied devices, which did play the role in energy level alignment of the ferromagnetic electrode/interface. Gobbi et al. [158] in 2011 presented significant room temperature MR values (in excess of 5%) on C60-based vertical spin valves for different thickness of the C60 interlayer (from 5 nm to 28 nm) up to high applied bias voltage (~1 V). Kawasugi et al. recently fabricated a TPD-based OSV (200 nm thickness) using Co_2MnSi Heusler alloy with large Tc to ensure a large spin injection at room temperature and measured nearly 10% MR in it [122]. Li et al. fabricated an OSV with the improved interface structure between the polymer interlayer and top cobalt electrode, optimal annealing of bottom manganite electrode, and a n-type semiconducting polymer P(NDI2OD-T2) having high carrier mobility, in which they measured a large MR ratio of 90.0% at 4.2 K and of 6.8% at room temperature, respectively [131]. The large MR at room temperature was attributed to the weak temperature dependence of spin diffusion length. The organic spintronic community is aggressively in search of a ferromagnetic electrode with high polarization [87,94] and OSCs with high spin-diffusion length [41,157] at room temperature. However, some recent research shows that improved "spinterface" should be prioritized to enhance the room temperature MR rather than only chasing the ideal materials and electrodes [44,45,166].

3.5. The role of FM/OSC contact in OSVs

The nature of FM electrode/organic spacer contact, or spinterface is crucial for the polarized spin injection that affects the magnitude of MR, voltage and temperature dependence of MR and the MR sign as well [19,59]. It is expected that such insights can lead to the molecular-level engineering of metal/organic interface not only to overcome the conductivity mismatch problem but also to customize spin injection as well for bringing new electrical functionalities to the spintronic devices. There have been existing two methods for surface induced spin polarization manipulation: a direct hybridization of the electron orbital between organics and metals, and tunneling barrier inclusion between a FM electrode and organics.

(i) First, although the conductivity mismatch has been thought to be less severe in OSVs since carriers are injected into the OSCs mainly by tunneling. A recent study by Barraud et al. [44] suggests that a proper OSC/FM interface can act as an excellent spin filter that can boost the effective spin polarization to even surpass the bulk spin polarization of the FM materials (Table 1) [167]. For examples, the effective spin

polarization of at the Co/Alq_3 interface extracted from Jullière's model for 300% TMR is about +60%, much higher than the 34% Co spin polarization. Barraud et al. suggested that the formation of localized states in the first molecular layer at the electrode interface can cause a spin dependent broadening of those states when coupled to the FM electrode. The sign of the effective spin polarization of the electrode and hence the magnitude of MR depend on how strong the coupling is. We note that availability of a practically infinite choice of organic molecules and functioning groups should boost up the confidence for a successful injection that so far has been difficult to achieve especially at room temperature [166]. Djeghlou et al. in 2013 observed a highly spin-polarized organic spinterface between Co and phthalocyanine molecules at room temperature by using the spin-polarized direct and inverse photoemission experiments [45]. The result suggests an exceptionally large MR response of more than 500%. The spinterface effect has been confirmed by several studies using first principle calculation to understand the effect of the orbital hybridization between molecules and FM electrodes on spin injection capability [166,168,169].

(ii) In addition to spinterface effect caused by the direct molecule/FM electrode couplling, Schulz et al. [170] showed that a thin polar insulating material such as LiF sandwiched between FM electrode and the organic layer can modify the extraction of charge carriers from an OSC leading to the MR sign change. It is worth noting that this method has been extensively studied to manipulate the charge injection in OLEDs and organic photovoltaics [171,172]. Similarly, Jiang et al. demonstrated that an asymmetric MR bias dependence can be amplified by studying the LSMO/Al_2O_3/Alq_3/Co spin valves [96]. Their simulation showed the origin of the bias dependence of MR might be related to the energy dependent density of states of Co d-states. It is worth noting that the tunneling barrier inclusion method has not shown an enhancement of the absolute interfacial spin polarization in comparison to the spin polarization of the bulk FM materials. Although the method does not show evidence for the spinterface enhancement, it does reveal that the effective spin polarization of the electrodes gets modified and even provides a sign reversal [87,170].

Strikingly, using interfaces between metallic films with a certain thickness and C60 molecule layer, Mari et al. recently demonstrated that it is possible to alter the electronic states of non-ferromagnetic materials, such as diamagnetic copper and paramagnetic manganese, to overcome the Stoner criterion for ferromagnetism and make them ferromagnetic at room temperature [173]. This is a direct proof of the crucial role of the molecule/metal interfaces in deciding ferromagnetism or effective spin polarization of the material. The mechanism suggests the exploitation of molecular coupling to design magnetic metamaterials using abundant, non-toxic components such as OSCs. The magnetic metamaterials might fill up the gap for the shortage of SP electron injectors from conventional magnetic materials for efficient bipolar spin valves such as spin-OLEDs.

3.6. Engineering of spin injection and transport using π-conjugated polymer brushes

We have so far reviewed the advances in understanding the spin injection and spin transport in conventional OSVs where the control in the spinterface is very limited due to a lack of robust device fabrication methods. In addition, the charge transport in these studies is mainly governed by the hopping transport with poor mobility. This limits the spin diffusion length to less than 200 nm as described in the previous section. Recently, Geng et al. [174] reported a novel fabrication method to better control the spinterface and mobility of the device. They used surface initiated Kumada transfer polycondensation method to covalently graft π-conjugated poly(3-methylthiophene) (P3MT) brushes from the LSMO bottom electrode. The covalent attachment along with the brush morphology allows the control over the LSMO/brush interfacial resistance and large spacer mobility (Fig. 7a). In principle, the interface resistance and hence spinterface can be manipulated by controlling the insulating alkyl spacer monolayer. Fig. 7b shows the device resistance versus the brush thickness. In general, the larger the device thickness, the larger the device resistance. The resistance of the P3MT brush-based device is much lower than that of the P3HT film-based device with a similar spacer thickness. We note that P3MT and P3HT have similar chemical structures and constituted elements, essentially causing the same spin-related-interactions including HFI and SOC. Remarkably, with 15 nm brush spacer layer, Geng et al. observed an optimum MR effect of 70% at cryogenic temperatures and a MR of 2.7% at 280 K, one of the best MR values reported at room temperature (Fig. 7c). Fig. 7d shows the temperature dependence of MR in P3MT brush-based device which is nearly an order of magnitude weaker than that found in the P3HT-based one. There are two scenarios for the weaker temperature dependence in the P3MT-based OSVs. (i) The introduction of the monolayer (tunnel barrier) for the covalent bond between the P3MT brush and the LSMO electrode may aid in overcoming the resistance mismatch problem at high temperature and therefore causes a weaker MR decay of the effective spin polarization at the LSMO interface [47,48,50,51]. As discussed in the previous sections, the resistance mismatch problem can be overcome by using either an appropriate insulator (spin filter) at the interface or an electrode material with 100% spin polarization [33]. The resistance mismatch problem, in principle, is suppressed at cryogenic temperature since the LSMO possesses nearly 100% spin polarization for both P3HT-base and P3MT-based OSVs. However, since LSMO has low Tc of about 350 K, the spin polarization is smaller at higher temperature and almost diminishes at room temperature. The tunnel barrier at high temperature may reduce the conductivity mismatch problem resulting in a better effective spin polarization of the LSMO electrode in the P3MT-based OSVs. (ii) The interfacial spin polarization of the LSMO might be modified during the monolayer deposition on the LSMO surface. However, the spin diffusion length of several 10 nm measured by the thickness dependence is not as large as expected by its superior large mobility over the corresponding polycrystalline films.

3.7. Challenges

There are challenging issues that need to be resolved. We highlight several major challenges in the section. (i) Organic semiconductors are among the softest, most chemically sensitive, and impure materials so that numerous factors during the material synthesis and device fabrication process can affect the spin injection/detection and transport in the device. These create challenges to achieve operational and reproducible devices. For instance, the quality of the organic spacer is strongly dependent on the morphology of the film, oxygen and moisture present in the film, metal contamination in the film during the fabrication process, high energy photon illumination such as X-ray illumination during the evaporation and the surface quality of the film as well [14,57,139,141,175]. Therefore, it is difficult to understand the charge hopping transport in OSCs whose density of states is not well-defined and with uncontrollable trap states. In fact, it is

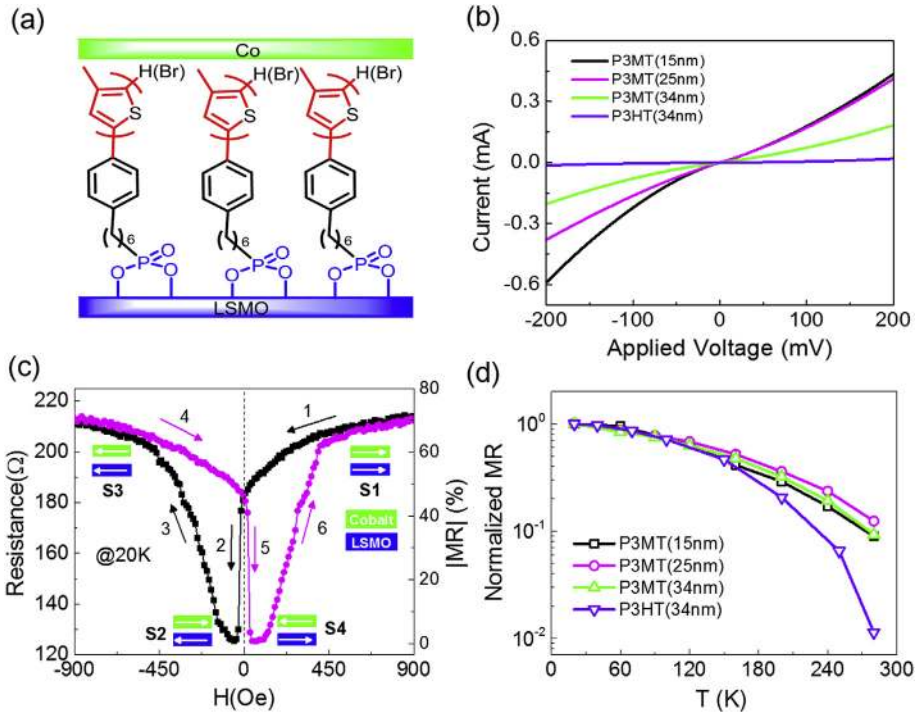

Fig. 7. Organic spin valves using π-conjugated polymer brushes as the interlayer. (a) Schematic diagram of the device cross section showing the polymer brushes covalently bound to the LSMO surface. (b) IV-characteristics of the OSVs measured at 20 K with different thicknesses of P3MT polymer brushes. The IV curve of P3HT-based OSV with 34 nm thickness is plotted together for comparison. (c) MR loops of P3HT polymer brush-based OSVs at low temperature. (d) Temperature dependence of the normalized MR of P3HT film-based OSV, and P3MT brush-based OSVs with various thicknesses. Reproduced with permission [174].

even much more difficult to understand the spin transport and spin dynamics including spin dephasing time and spin relaxation time in such system. Based on several fundamental problems and controversial experimental results in OSVs, a spin dynamic theory based on spin-charge decoupling was proposed by Yu [160,176]. For example, the small mobility and hence the spin diffusion length of the charge transport in OSCs has been an obvious obstacle for observing the spin precession or Hanle effect in the materials. This is the most convincing and elegant verification for the existence of spin transport and spin dynamics in spin transport materials. We note that the study of the Hanle effect normally prefers to the spin valve with a non-local planar device structure, in which the spin current can be decoupled with electric current to reduce the complication of various spurious effects caused by the drift current [177,178]. However, due to the small spin diffusion length of organics, the demonstration of such phenomenon is technologically challenging. Even when the pure spin current is generated by FMR spin pumping method as described in the previous sections, the observation of Hanle effect in organics is still under debate [17,137]. The complication comes from the presence of the large DC magnetic field for the FMR spin pump. In addition, despite the spurious effects, there have been several unsuccessful demonstrations of Hanle effect experiments in vertical OSVs using amorphous OSC films [179,180] (Fig. 8b). The absence of the Hanle effect in those attempts was explained by the fact that the transit time across the device is much larger than the spin precession time. (ii) In addition the challenges of the spin transports in OSCs, the current fabrication methods for the top metal electrode in OSVs normally generate a metal inclusion whose depth depends on the organic and FM materials used and the evaporation conditions. Since the concept of epitaxial growth does not so far exist in OSCs, the contact between organics and FM electrodes is poorly controlled leading to challenges in controlling the spinterface. The poor FM/OSC contacts especially from the top one might create many spin transport channels with different lengths in OSCs causing different spin dephasing angles at the spin detector. This reason simply smears the observation of the Hanle effect in OSVs.

Despite all of these difficulties belonging to the material properties and device fabrication, the motivation for utilizing OSCs as host for SP charge carriers relies on their weak SOC and HFI which are the source for spin-dephasing and spin relaxation. However, the weak SOC in OSCs also creates difficulties in using optical means, such as spin pumping or detecting by circularly polarized light to probe the spin injection in OSCs. In addition, the excitonic nature of polaronic electron–hole pairs in organics might make the spins lose their memory before the radiation recombination. Such optical spin injection/detection has not been reported in organic materials.

4. Spin-OLEDs

In the Section 3, we discussed the major advances and challenges in OSVs during at least the last 10 years. In this type of device, only one SP hole is considered since most FM materials have workfunctions close to the organic molecule HOMO energy levels. In this section, a new class of OSVs, dubbed bipolar OSVs or spin-OLEDs will be reviewed. In this device, SP electrons and holes from FM electrodes are injected into the LUMO and HOMO energy levels of an organic emissive layer, respectively, causing electroluminescence (EL) [59,181,182]. A spin-OLED is basically an OSV that allows the injection of both SP electrons and holes into the organic spacer (Fig. 9a). To obtain the luminescence, the applied voltage must be larger than the band gap of the OSC spacer and one of FM electrodes must be used for injecting SP electrons into the LUMO energy level. In these devices, the singlet exciton density and hence EL intensity can be controlled by manipulating the relative

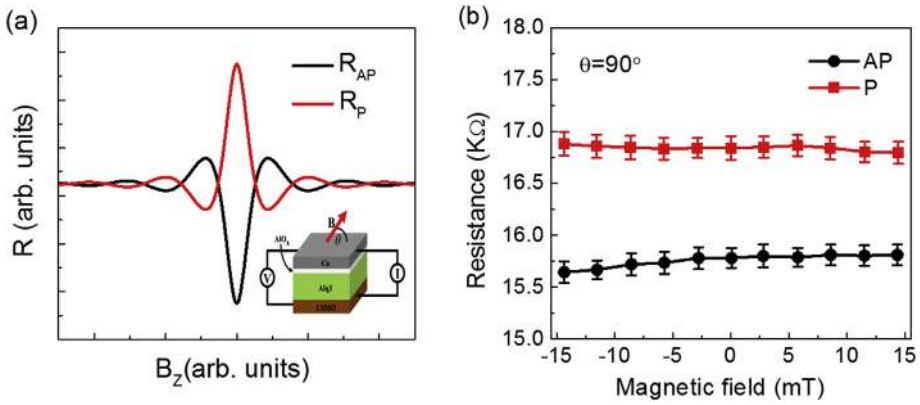

Fig. 8. Missing Hanle effect in OSVs. (a) Simulation of the parallel resistance and antiparallel resistance of an OSV as a function of the perpendicular magnetic field. (b) Resistance of an OSV as a function of perpendicular magnetic field measured by Riminucci et al. [179] Inset of (a) is the schematic of the OSV used by Riminucci et al. for the Hanle effect study. Reproduced with permission [179].

magnetization of the two FM electrodes [182]. In the ideal operating condition that uses 100% SP electron and hole injectors, and infinite spin diffusion length OSCs, one can turn the device emission from off-state with no light to on-state with 50% quantum efficiency. In addition, this effect in the bipolar OSVs can be utilized to detect the spin polarization of the injected carriers and also to potentially control the color of the EL emission [18,182]. Recently, Nguyen et al. fabricated spin-OLED devices using deuterated DOO-PPV (Fig. 1) with about 50 nm spin diffusion length as the emissive interlayer sandwiched between the LSMO anode and CO/LiF cathode; and studied the magneto-conductance (MC) and magneto-electroluminescence (MEL) effects [182]. Since the Co has a work function as high as that in LSMO (about 4.7 eV), a thin electric polar LiF layer was applied at the Co interface to reduce the interfacial work function of Co, suitable for SP electron injection. The use of LiF for manipulating the interfacial work function for the electron injection has been extensively used in organic solar cells [183]. However, there is a trade-off for this action since the effective spin polarization of Co electrode reduces substantially [170]. Therefore, the spin-OLED response in the device is expected to be small. Fig. 9b shows the bipolar IV behavior of spin OLEDs where the emission appears roughly at the turn-on applied voltage for the current. Fig. 9c shows a typical MEL hysteretic loop of the spin valve device for sweeping of external magnetic field at 4.5 V bias voltage and 10 K temperature. The switching in the high and low states of the MEL corresponded to the coercive fields of the FM electrodes indicating its origination from the bipolar spin-polarization. The normalized MC magnitude up to 6.0 V of the device (red line) is shown Fig. 9d. The fast reduction of the MR or MC response below 3.0 V bias is commonly seen in the spin valve response (blue line in Fig. 9d). We note that the spin-OLED response under an applied magnetic field is quite complicated in the bipolar regime, since the magnetic field can also alter the singlet and triplet exciton formation causing the non-hysteretic OMAR effect [181].

One of the serious obstacles for preventing the application of spin-OLEDs is the strong reduction of the MR at high bias voltages. The MR in OSVs has been found up to 300% but normally diminishes at the junction voltage of less than 3 V (see Fig. 8d). The reduction can be attributed to the reduction of the spin polarization and/or spin diffusion length at increased bias voltage. Therefore, novel materials for both spin injectors and organic interlayers need to be discovered. It is worth mentioning the other kind of spin valve structure, namely the double layer magnetic tunnel junction (see Fig. 10a) that has been known to operate at higher junction voltages [184]. Liang et al. [185] recently achieved 0.3% MR effect in the Alq_3-based double layer OSVs with -6 V bias voltage at low temperature (i.e. 10 K) (see Fig. 10b). The mechanism associated with this high voltage MR response in OSVs has not been investigated.

5. Summary and outlook

In the above sections, we provided a thorough review on major achievements and challenges in OSVs and spin-OLEDs with an emphasis on experimental findings during the last decade [165]. Although OSVs are very promising for the plastic spintronic applications with cost efficiency, there are many technological and fundamental issues that need to be overcome and addressed. To mature the field further, multiple actions need to be pursued and novel techniques have to be developed beyond the conventional OSV material, fabrication and characterization. These push continued search for finding novel spin injection/detection for OSVs with spin polarization close to 100% at high T_C; with high chemical stability; novel organic spin transport materials, appropriate device fabrication strategies for more controllability of the spinterface and morphology of the spacer; and novel device structures similar to the non-local spin valve device for generating the pure spin current in order to gain deeper fundamental understanding of the spin transport in OSCs. As an approach for novel spin transport materials, OSCs such as organic single crystals and aligned polymers which have relatively high carrier mobility for the spin transport layer might be discovered and used for fabrication of novel OSVs. In addition, since such materials have a much simpler density of states than conventional OSVs, they are more suitable for the fundamental studies of spin transport. For example, the mobility of a typical rubrene single crystal is about ~20 cm^2/Vs at 300 K, several orders of magnitude higher than that of the amorphous rubrene [186,187]. In addition, the intra-chain mobility of charge carriers in the polymer has been inferred as high as 30 cm^2/Vs from measurements of ladder-type polymers desirable for using π-conjugated polymer brushes as the spacer for OSVs [188]. Therefore, a large spin diffusion length is expected to be several orders of magnitude longer in these materials, showing the potential for the advancement of organic spintronics. If the long spin diffusion is verified, the non-local spin valve structure and hence Hanle effect might be realized. Perhaps, this is one of the most convincing experimental designs for studying the spin transport properties of the spacer where the connection between spin diffusion length, charge mobility and spin relaxation time are well

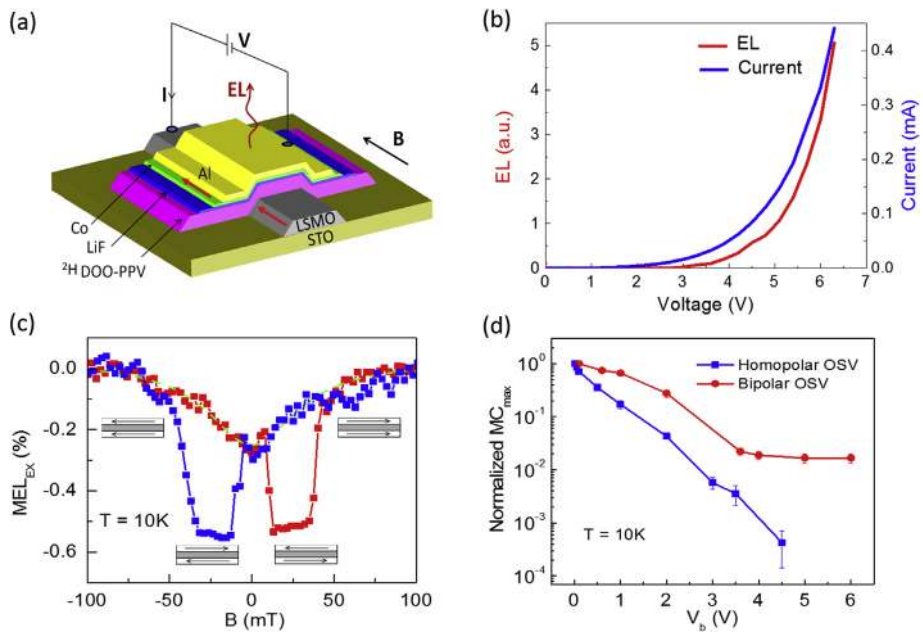

Fig. 9. Spin-polarized OLED based on organic bipolar spin valves. (a) The schematic of the device structure. (b) The device I–V and EL-V characteristics. (c) Magneto-electroluminescence (MEL) response of the device. (d) Bias voltage dependence of the normalized MC of bipolar and homopolar device. Reproduced with permission [182].

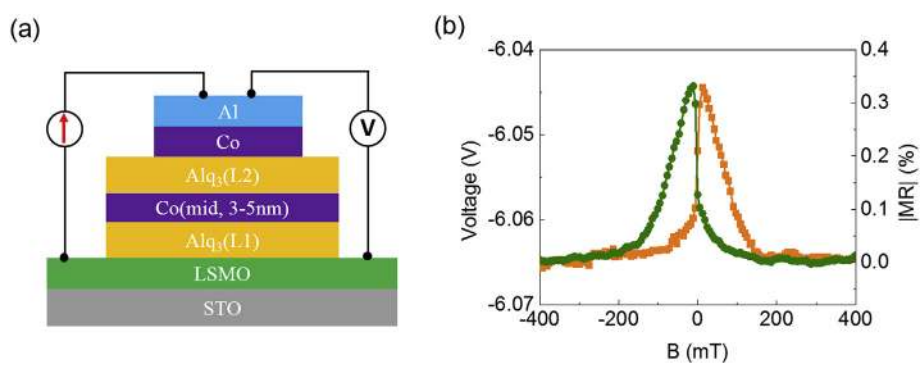

Fig. 10. (a) The schematic of a double-layer OSV fabricated by Liang et al. in their study. (b) Measured MR with large bias voltage of −6 V at low temperature. Reproduced with permission [185].

established in inorganic spintronics [20,177,178,189–191]. In addition to the quest for novel organic spin transport materials, the FM materials with high chemical stability and high TC need to be discovered. So far, most of the MR reports in OSVs used either high chemical sensitivity electrodes such as Fe, Co or the alloys or/and half-metals such as LSMO with nearly 100% spin polarization at low temperature but with low Tc. The novel half-metal oxides with high T_C are preferred since it satisfies the above criteria. Heusler alloy such as Co_2MnSi with $T_C = 985$ K and nearly 100% spin polarization appears to be a good candidate [81,122]. In addition, the controllability of the spinterface effect is needed since the electron hybridization might significantly alter the effective spin polarization of the electrodes. Unfortunately, the nature of organic/metal contacts using either thermal evaporation or solution processing fabrication methods is poorly controlled thus far. Because the epitaxial growth technology of organic materials on metal surfaces does not exist, a possible way to control the interface is to chemically grow a self-assembled monolayer (SAM) on the magnetic electrodes. This type of SAM controlled spinterface effect in π-conjugated polymer brush-based OSVs has recently been achieved by Geng et al. [174].

Acknowledgements

This work was supported in part by University of Georgia start-up funds and Faculty Research Grant (T.N.), as well as startup funds provided by the UGA College of Engineering (L.A.H).

References

[1] W.P. Su, J.R. Schrieffer, A.J. Heeger, Solitons in polyacetylene, Phys. Rev. Lett. 42 (1979) 1698–1701.
[2] C.W. Tang, Two-layer organic photovoltaic cell, Appl. Phys. Lett. 48 (1986) 183–185.
[3] C.W. Tang, S.A. VanSlyke, Organic electroluminescent diodes, Appl. Phys. Lett. 51 (1987) 913–915.
[4] R.J. Elliott, Spin-orbit coupling in band theory-character tables for some "double" space groups, Phys. Rev. 96 (1954) 280–287.
[5] Y. Yafet, g Factors and spin-lattice relaxation of conduction electrons, in: S. Frederick, T. David (Eds.), Solid State Phys, Academic Press, 1963, pp. 1–98.
[6] M.I. D'Yakonov, V.I. Perel', Spin orientation of electrons associated with the interband absorption of light in semiconductors, Sov. Phys. JETP 33 (1971) 1053.
[7] I. Žutić, J. Fabian, S. Das Sarma, Spintronics: fundamentals and applications, Rev. Mod. Phys. 76 (2004) 323–410.
[8] W.J.M. Naber, S. Faez, W.G. van der Wiel, Organic spintronics, J. Phys. D. 40 (2007) R205–R228.

[9] R. Geng, T.T. Daugherty, K. Do, H. Luong, T.D. Nguyen, A Review on Organic Spintronic Materials and Devices: I. Magnetic Field Effect on Organic Light Emitting Diodes, J. Sci. Adv. Mater. Devices 1 (2016) 128–140.
[10] M. Oestreich, M. Bender, J. Hübner, D. Hägele, W.W. Rühle, H. Th, P.J. Klar, W. Heimbrodt, M. Lampalzer, K. Volz, W. Stolz, Spin injection, spin transport and spin coherence, Semicond. Sci. Technol. 17 (2002) 285.
[11] R.R. Parsons, Band-to-band optical pumping in solids and polarized photoluminescence, Phys. Rev. Lett. 23 (1969) 1152–1154.
[12] M. Cinchetti, K. Heimer, J. Wüstenberg, O. Andreyev, M. Bauer, S. Lach, C. Ziegler, Y. Gao, M. Aeschlimann, Determination of spin injection and transport in a ferromagnet/organic semiconductor heterojunction by two-photon photoemission, Nat. Mater. 8 (2009) 115–119.
[13] H. Ding, Y. Gao, M. Cinchetti, J.-P. Wüstenberg, M. Sánchez-Albaneda, O. Andreyev, M. Bauer, M. Aeschlimann, Spin injection and spin dynamics at the CuPc/GaAs interface studied with ultraviolet photoemission spectroscopy and two-photon photoemission spectroscopy, Phys. Rev. B 78 (2008) 075311.
[14] Z.H. Xiong, D. Wu, Z.V. Vardeny, J. Shi, Giant magnetoresistance in organic spin-valves, Nature 427 (2004) 821–824.
[15] Y. Ohno, D.K. Young, B. Beschoten, F. Matsukura, H. Ohno, D.D. Awschalom, Electrical spin injection in a ferromagnetic semiconductor heterostructure, Nature 402 (1999) 790–792.
[16] K. Ando, S. Takahashi, J. Ieda, Y. Kajiwara, H. Nakayama, T. Yoshino, K. Harii, Y. Fujikawa, M. Matsuo, S. Maekawa, E. Saitoh, Inverse spin-Hall effect induced by spin pumping in metallic system, J. Appl. Phys. 109 (2011) 103913.
[17] S. Watanabe, K. Ando, K. Kang, S. Mooser, Y. Vaynzof, H. Kurebayashi, E. Saitoh, H. Sirringhaus, Polaron spin current transport in organic semiconductors, Nat. Phys. 10 (2014) 308.
[18] D.L. Sun, E. Ehrenfreund, Z.V. Vardeny, The first decade of organic spintronics research, Chem. Commun. 50 (2014) 1781–1793.
[19] A.J. Drew, J. Hoppler, L. Schulz, F.L. Pratt, P. Desai, P. Shakya, T. Kreouzis, W.P. Gillin, A. Suter, N.A. Morley, V.K. Malik, A. Dubroka, K.W. Kim, H. Bouyanfif, F. Bourqui, C. Bernhard, R. Scheuermann, G.J. Nieuwenhuys, T. Prokscha, E. Morenzoni, Direct measurement of the electronic spin diffusion length in a fully functional organic spin valve by low-energy muon spin rotation, Nat. Mater. 8 (2009) 109–114.
[20] X. Lou, C. Adelmann, S.A. Crooker, E.S. Garlid, J. Zhang, K.S.M. Reddy, S.D. Flexner, C.J. Palmstrom, P.A. Crowell, Electrical detection of spin transport in lateral ferromagnet-semiconductor devices, Nat. Phys. 3 (2007) 197–202.
[21] M. Kepenekian, R. Robles, C. Katan, D. Sapori, L. Pedesseau, J. Even, Rashba and dresselhaus effects in hybrid organic–inorganic perovskites: from basics to devices, ACS Nano (2015) 11557–11567.
[22] N. Baadji, M. Piacenza, T. Tugsuz, F.D. Sala, G. Maruccio, S. Sanvito, Electrostatic spin crossover effect in polar magnetic molecules, Nat. Mater. 8 (2009) 813–817.
[23] C.C. Lo, J. Li, I. Appelbaum, J.J.L. Morton, Microwave manipulation of electrically injected spin-polarized electrons in silicon, Phys. Rev. Appl. 1 (2014) 014006.
[24] E. Shikoh, K. Ando, K. Kubo, E. Saitoh, T. Shinjo, M. Shiraishi, Spin-pump-induced spin transport in p-Type Si at room temperature, Phys. Rev. Lett. 110 (2013) 127201.
[25] R. Fiederling, M. Keim, G. Reuscher, W. Ossau, G. Schmidt, A. Waag, L.W. Molenkamp, Injection and detection of a spin-polarized current in a light-emitting diode, Nature 402 (1999) 787–790.
[26] J.M. Kikkawa, I.P. Smorchkova, N. Samarth, D.D. Awschalom, Room-temperature spin memory in two-dimensional electron gases, Science 277 (1997) 1284–1287.
[27] A. Joshua, V. Venkataraman, Enhanced sensitivity in detection of Kerr rotation by double modulation and time averaging based on Allan variance, Rev. Sci. Instrum. 80 (2009) 023908.
[28] Y.K. Kato, R.C. Myers, A.C. Gossard, D.D. Awschalom, Observation of the spin hall effect in semiconductors, Science 306 (2004) 1910–1913.
[29] T. Jungwirth, J. Wunderlich, K. Olejnik, Spin Hall effect devices, Nat. Mater. 11 (2012) 382–390.
[30] M. Baibich, J.M. Broto, A. Fert, F. NguyenVanDan, F. Petroff, P. Etienne, G. Creuzert, A. Friederich, J. Chazelas, Giant magnetoresistance of (001)Fe/(001)Cr magnetic superlattices, Phys. Rev. Lett. 61 (1988) 2472–2475.
[31] V.P. LaBella, D.W. Bullock, Z. Ding, C. Emery, A. Venkatesan, W.F. Oliver, G.J. Salamo, P.M. Thibado, M. Mortazavi, Spatially resolved spin-injection probability for gallium arsenide, Science 292 (2001) 1518–1521.
[32] R. Laiho, H.J. Reittu, Spin-polarized scanning tunnelling microscopy with detection of polarized luminescence emerging from a semiconductor tip, J. Phys. Condens. Matter 9 (1997) 5697.
[33] S. Sanvito, Molecular spintronics, Chem. Soc. Rev. 40 (2011) 3336–3355.
[34] A.J. Drew, G. Szulczewski, L. Nuccio, W.P. Gillin, The role of interfaces in organic spin valves revealed through spectroscopic and transport measurements, Phys. Status Solidi B 249 (2012) 9–17.
[35] S. Sanvito, A.R. Rocha, Molecular-spintronics: the art of driving spin through molecules, J. Comput. Theor. Nanos. 3 (2006) 624.
[36] T.D. Nguyen, G. Hukic-Markosian, F. Wang, L. Wojcik, X. Li, E. Ehrenfreund, Z.V. Vardeny, Isotope effect in spin response of π-conjugated polymer films and devices, Nat. Mater. 9 (2010) 345–352.
[37] P.A. Bobbert, W. Wagemans, F.W.A.v. Oost, B. Koopmans, M. Wohlgenannt, Theory for spin diffusion in disordered organic semiconductors, Phys. Rev. Lett. 102 (2009) 156604.
[38] Z.G. Yu, Spin-orbit coupling, spin relaxation, and spin diffusion in organic solids, Phys. Rev. Lett. 106 (2011) 106602.
[39] Z.G. Yu, F. Ding, H. Wang, Hyperfine interaction and its effects on spin dynamics in organic solids, Phys. Rev. B 87 (2013) 205446.
[40] T.D. Nguyen, T.P. Basel, Y.J. Pu, X.G. Li, E. Ehrenfreund, Z.V. Vardeny, Isotope effect in the spin response of aluminum tris(8-hydroxyquinoline) based devices, Phys. Rev. B 85 (2012) 245437.
[41] J.H. Shim, K.V. Raman, Y.J. Park, T.S. Santos, G.X. Miao, B. Satpati, J.S. Moodera, Large spin diffusion length in an amorphous organic semiconductor, Phys. Rev. Lett. 100 (2008) 226603.
[42] G. Wang, B.L. Liu, A. Balocchi, P. Renucci, C.R. Zhu, T. Amand, C. Fontaine, X. Marie, Gate control of the electron spin-diffusion length in semiconductor quantum wells, Nat. Commun. 4 (2013).
[43] M. Julliere, Tunneling between ferromagnetic-films, Phys. Lett. A 54 (1975) 225–226.
[44] C. Barraud, P. Seneor, R. Mattana, S. Fusil, K. Bouzehouane, C. Deranlot, P. Graziosi, L. Hueso, I. Bergenti, V. Dediu, F. Petroff, A. Fert, Unravelling the role of the interface for spin injection into organic semiconductors, Nat. Phys. 6 (2010) 615–620.
[45] F. Djeghloul, F. Ibrahim, M. Cantoni, M. Bowen, L. Joly, S. Boukari, P. Ohresser, F. Bertran, P. Le Fèvre, P. Thakur, F. Scheurer, T. Miyamachi, R. Mattana, P. Seneor, A. Jaafar, C. Rinaldi, S. Javaid, J. Arabski, J.P. Kappler, W. Wulfhekel, N.B. Brookes, R. Bertacco, A. Taleb-Ibrahimi, M. Alouani, E. Beaurepaire, W. Weber, Direct observation of a highly spin-polarized organic spinterface at room temperature, Sci. Rep. 3 (2013) 1272.
[46] S. Sanvito, Organic electronics: spintronics goes plastic, Nat. Mater. 6 (2007) 803–804.
[47] D.L. Smith, R.N. Silver, Electrical spin injection into semiconductors, Phys. Rev. B 64 (2001) 045323.
[48] J.D. Albrecht, D.L. Smith, Electron spin injection at a Schottky contact, Phys. Rev. B 66 (2002) 113303.
[49] F.J. Wang, Z.H. Xiong, D. Wu, J. Shi, Z.V. Vardeny, Organic spintronics: the case of Fe/Alq_3/Co spin-valve devices, Synth. Met. 155 (2005) 172–175.
[50] M. Yunus, P.P. Ruden, D.L. Smith, Ambipolar electrical spin injection and spin transport in organic semiconductors, J. Appl. Phys. 103 (2008) 103714.
[51] E.I. Rashba, Theory of electrical spin injection: tunnel contacts as a solution of the conductivity mismatch problem, Phys. Rev. B 62 (2000) R16267–R16270.
[52] A.T. Hanbicki, B.T. Jonker, G. Itskos, G. Kioseoglou, A. Petrou, Efficient electrical spin injection from a magnetic metal/tunnel barrier contact into a semiconductor, Appl. Phys. Lett. 80 (2002) 1240–1242.
[53] C. Adelmann, X. Lou, J. Strand, C.J. Palmstrøm, P.A. Crowell, Spin injection and relaxation in ferromagnet-semiconductor heterostructures, Phys. Rev. B 71 (2005) 121301.
[54] V.F. Motsnyi, J. De Boeck, J. Das, W. Van Roy, G. Borghs, E. Goovaerts, V.I. Safarov, Electrical spin injection in a ferromagnet/tunnel barrier/semiconductor heterostructure, Appl. Phys. Lett. 81 (2002) 265–267.
[55] I.D. Parker, Carrier tunneling and device characteristics in polymer light-emitting diodes, J. Appl. Phys. 75 (1994) 1656–1666.
[56] M. Grünewald, N. Homonnay, J. Kleinlein, G. Schmidt, Voltage-controlled oxide barriers in organic/hybrid spin valves based on tunneling anisotropic magnetoresistance, Phys. Rev. B 90 (2014) 205208.
[57] S. Majumdar, R. Laiho, P. Laukkanen, I.J. Väyrynen, H.S. Majumdar, R. Österbacka, Application of regioregular polythiophene in spintronic devices: effect of interface, Appl. Phys. Lett. 89 (2006) 122114.
[58] D. Wu, Z.H. Xiong, X.G. Li, Z.V. Vardeny, J. Shi, Magnetic-field-dependent carrier injection at $La_{2/3}Sr_{1/3}MnO_3$ and organic semiconductors interfaces, Phys. Rev. Lett. 95 (2005) 016802.
[59] V.A. Dediu, L.E. Hueso, I. Bergenti, C. Taliani, Spin routes in organic semiconductors, Nat. Mater. 8 (2009) 707–716.
[60] M. Bibes, A. Barthelemy, Oxide spintronics, IEEE Trans. Electron Devices 54 (2007) 1003–1023.
[61] J.H. Park, E. Vescovo, H.J. Kim, C. Kwon, R. Ramesh, T. Venkatesan, Magnetic properties at surface boundary of a half-metallic ferromagnet $La_{0.7}Sr_{0.3}MnO_3$, Phys. Rev. Lett. 81 (1998) 1953–1956.
[62] J.W. Yoo, C.Y. Chen, H.W. Jang, C.W. Bark, V.N. Prigodin, C.B. Eom, A.J. Epstein, Spin injection/detection using an organic-based magnetic semiconductor, Nat. Mater. 9 (2010) 638–642.
[63] B. Li, C.-Y. Kao, J.-W. Yoo, V.N. Prigodin, A.J. Epstein, Magnetoresistance in an all-organic-based spin valve, Adv. Mater. 23 (2011) 3382–3386.
[64] V.N. Prigodin, J.W. Yoo, H.W. Jang, C. Kao, C.B. Eom, A.J. Epstein, New advances in organic spintronics, J. Phys. Conf. Ser. 292 (2011) 012001.
[65] J.S. Miller, Organic- and molecule-based magnets, Mater. Today 17 (2014) 224–235.
[66] M. Bowen, M. Bibes, A. Barthélémy, J.-P. Contour, A. Anane, Y. Lemaître, A. Fert, Nearly total spin polarization in $La_{2/3}Sr_{1/3}MnO_3$ from tunneling experiments, Appl. Phys. Lett. 82 (2003) 233–235.
[67] P.M. Tedrow, R. Meservey, Spin polarization of electrons tunneling from films of Fe, Co, Ni, and Gd, Phys. Rev. B 7 (1973) 318–326.
[68] C.M. Schneider, P. Bressler, P. Schuster, J. Kirschner, J.J. de Miguel, R. Miranda, Curie temperature of ultrathin films of fcc-cobalt epitaxially grown on atomically flat Cu(100) surfaces, Phys. Rev. Lett. 64 (1990) 1059–1062.
[69] H.B. Michaelson, The work function of the elements and its periodicity, J. Appl. Phys. 48 (1977) 4729–4733.
[70] S. Velasco, F.L. Román, Determining the Curie temperature of iron and nickel, Phys. Teach. 45 (2007) 387–389.

[71] D.J. Monsma, S.S.P. Parkin, Spin polarization of tunneling current from ferromagnet/Al_2O_3 interfaces using copper-doped aluminum superconducting films, Appl. Phys. Lett. 77 (2000) 720–722.
[72] T. Löfwander, R. Grein, M. Eschrig, Is CrO_2 fully spin Polarized? Analysis of andreev spectra and excess current, Phys. Rev. Lett. 105 (2010) 207001.
[73] J.J. Attema, M.A. Uijttewaal, G.A. de Wijs, R.A. de Groot, Work function anisotropy and surface stability of half-metallic CrO_2, Phys. Rev. B 77 (2008) 165109.
[74] J.S. Kouvel, D.S. Rodbell, Magnetic critical-point behavior of CrO_2, J. Appl. Phys. 38 (1967) 979–981.
[75] N.A. Morley, A. Rao, D. Dhandapani, M.R.J. Gibbs, M. Grell, T. Richardson, Room temperature organic spintronics, J. Appl. Phys. 103 (2008) 07F306.
[76] T. Sourmail, Near equiatomic FeCo alloys: constitution, mechanical and magnetic properties, Prog. Mater. Sci. 50 (2005) 816–880.
[77] Y.S. Dedkov, U. Rüdiger, G. Güntherodt, Evidence for the half-metallic ferromagnetic state of Fe_3O_4 by spin-resolved photoelectron spectroscopy, Phys. Rev. B 65 (2002) 064417.
[78] K. Hild, J. Maul, T. Meng, M. Kallmayer, G. Schonhense, H.J. Elmers, R. Ramos, S.K. Arora, I.V. Shvets, Optical magnetic circular dichroism in threshold photoemission from a magnetite thin film, J. Phys. Condens. Matter 20 (2008) 235218.
[79] H. Xiang, F. Shi, M.S. Rzchowski, P.M. Voyles, Y.A. Chang, Epitaxial growth and magnetic properties of Fe3O4 films on TiN buffered Si(001), Si(110), and Si(111) substrates, Appl. Phys. Lett. 97 (2010) 092508.
[80] J.F. Sierra, V.V. Pryadun, S.E. Russek, M. Garcia-Hernandez, F. Mompean, R. Rozada, O. Chubykalo-Fesenko, E. Snoeck, G.X. Miao, J.S. Moodera, F.G. Aliev, Interface and temperature dependent magnetic properties in permalloy thin films and tunnel junction structures, J. Nanosci. Nanotechnol. 11 (2011) 7653–7664.
[81] M. Jourdan, J. Minár, J. Braun, A. Kronenberg, S. Chadov, B. Balke, A. Gloskovskii, M. Kolbe, H.J. Elmers, G. Schönhense, H. Ebert, C. Felser, M. Kläui, Direct observation of half-metallicity in the Heusler compound Co_2MnSi, Nat. Commun. 5 (2014) 3974.
[82] F. Roman, O. Siham, H. Yusuke, L. Hong-xi, C. Stanislav, B. Benjamin, U. Shigenori, S. Motohiro, U. Tetsuya, Y. Masafumi, A. Martin, C. Mirko, H.F. Gerhard, F. Claudia, Spin-resolved low-energy and hard x-ray photoelectron spectroscopy of off-stoichiometric Co_2MnSi Heusler thin films exhibiting a record TMR, J. Phys. D. Appl. Phys. 48 (2015) 164002.
[83] P.J. Brown, K.U. Neumann, P.J. Webster, K.R.A. Ziebeck, The magnetization distributions in some Heusler alloys proposed as half-metallic ferromagnets, J. Phys. Condens. Matter 12 (2000) 1827.
[84] V. Dediu, M. Murgia, F.C. Matacotta, C. Taliani, S. Barbanera, Room temperature spin polarized injection in organic semiconductor, Solid State Commun. 122 (2002) 181–184.
[85] F. Wang, Z.V. Vardeny, Recent advances in organic spin-valve devices, Synth. Met. 160 (2010) 210–215.
[86] J. Devkota, R. Geng, R.C. Subedi, T.D. Nguyen, Organic spin valves: a review, Adv. Funct. Mater. 26 (2016) 3881–3898.
[87] V. Dediu, Room-temperature spintronic effects in Alq3-based hybrid devices, Phys. Rev. B 78 (2008) 115203.
[88] W. Xu, G.J. Szulczewski, P. LeClair, I. Navarrete, R. Schad, G.X. Miao, H. Guo, A. Gupta, Tunneling magnetoresistance observed in $La_{0.67}Sr_{0.33}MnO_3$/organic molecule/Co junctions, Appl. Phys. Lett. 90 (2007) 072506.
[89] H. Vinzelberg, J. Schumann, D. Elefant, R.B. Gangineni, J. Thomas, B. Büchner, Low temperature tunneling magnetoresistance on (La,Sr)MnO_3/Co junctions with organic spacer layers, J. Appl. Phys. 103 (2008) 093720.
[90] S. Majumdar, H.S. Majumdar, R. Laiho, R. Österbacka, Comparing small molecules and polymer for future organic spin-valves, J. Alloys Compd. 423 (2006) 169–171.
[91] T.S. Santos, J.S. Lee, P. Migdal, I.C. Lekshmi, B. Satpati, J.S. Moodera, Room-temperature tunnel magnetoresistance and spin-polarized tunneling through an organic semiconductor barrier, Phys. Rev. Lett. 98 (2007) 016601.
[92] D. Sun, L. Yin, C. Sun, H. Guo, Z. Gai, X.G. Zhang, T.Z. Ward, Z. Cheng, J. Shen, Giant magnetoresistance in organic spin valves, Phys. Rev. Lett. 104 (2010) 236602.
[93] J. De Teresa, A. Barthélémy, A. Fert, J. Contour, R. Lyonnet, F. Montaigne, P. Seneor, A. Vaures, Inverse tunnel magnetoresistance in Co/$SrTiO_3$/$La_{0.7}Sr_{0.3}MnO_3$: new ideas on spin-polarized tunneling, Phys. Rev. Lett. 82 (1999) 4288.
[94] F.J. Wang, C.G. Yang, Z.V. Vardeny, X.G. Li, Spin response in organic spin valves based on $La_{2/3}Sr_{1/3}MnO_3$ electrodes, Phys. Rev. B 75 (2007) 7.
[95] J.S. Moodera, G. Mathon, Spin polarized tunneling in ferromagnetic junctions, J. Magn. Magn. Mater. 200 (1999) 248–273.
[96] S.W. Jiang, D.J. Shu, L. Lin, Y.J. Shi, J. Shi, H.F. Ding, J. Du, M. Wang, D. Wu, Strong asymmetrical bias dependence of magnetoresistance in organic spin valves: the role of ferromagnetic/organic interfaces, New J. Phys. 16 (2014) 013028.
[97] J. Zhang, R.M. White, Voltage dependence of magnetoresistance in spin dependent tunneling junctions, J. Appl. Phys. 83 (1998) 6512–6514.
[98] Y. Zheng, F. Wudl, Organic spin transporting materials: present and future, J. Mater. Chem. A 2 (2014) 48–57.
[99] M. Grünewald, M. Wahler, F. Schumann, M. Michelfeit, C. Gould, R. Schmidt, F. Würthner, G. Schmidt, L.W. Molenkamp, Tunneling anisotropic magnetoresistance in organic spin valves, Phys. Rev. B 84 (2011) 125208.
[100] J.-W. Yoo, H.W. Jang, V.N. Prigodin, C. Kao, C.B. Eom, A.J. Epstein, Tunneling vs. giant magnetoresistance in organic spin valve, Synth. Met. 160 (2010) 216–222.
[101] T.L.A. Tran, T.Q. Le, J.G.M. Sanderink, W.G. van der Wiel, M.P. de Jong, The multistep tunneling analogue of conductivity mismatch in organic spin valves, Adv. Funct. Mater. 22 (2012) 1180–1189.
[102] J.J.H.M. Schoonus, P.G.E. Lumens, W. Wagemans, J.T. Kohlhepp, P.A. Bobbert, H.J.M. Swagten, B. Koopmans, Magnetoresistance in hybrid organic spin valves at the onset of multiple-step tunneling, Phys. Rev. Lett. 103 (2009) 146601.
[103] C. Barraud, C. Deranlot, P. Seneor, R. Mattana, B. Dlubak, S. Fusil, K. Bouzehouane, D. Deneuve, F. Petroff, A. Fert, Magnetoresistance in magnetic tunnel junctions grown on flexible organic substrates, Appl. Phys. Lett. 96 (2010) 072502.
[104] G. Narjes, Q. Su Ying, Interface effects on tunneling magnetoresistance in organic spintronics with flexible amine–Au links, Nanotechnology 24 (2013) 415201.
[105] G. Horowitz, F. Garnier, A. Yassar, R. Hajlaoui, F. Kouki, Field-effect transistor made with a sexithiophene single crystal, Adv. Mater. 8 (1996) 52–54.
[106] B. Park, J. Park, Charge-transfer-induced doping at an electron donor (α-sexithiophene)/acceptor (C60) interface and mobility improvement, Phys. Status Solidi RRL 8 (2014) 74–80.
[107] H. Park, D.-S. Shin, H.-S. Yu, H.-B. Chae, Electron mobility in tris(8-hydroxyquinoline)aluminum (Alq_3) films by transient electroluminescence from single layer organic light emitting diodes, Appl. Phys. Lett. 90 (2007) 202103.
[108] W. Brütting, H. Riel, T. Beierlein, W. Riess, Influence of trapped and interfacial charges in organic multilayer light-emitting devices, J. Appl. Phys. 89 (2001) 1704–1712.
[109] D.H. Kim, Y.D. Park, Y. Jang, H. Yang, Y.H. Kim, J.I. Han, D.G. Moon, S. Park, T. Chang, C. Chang, M. Joo, C.Y. Ryu, K. Cho, Enhancement of field-effect mobility due to surface-mediated molecular ordering in regioregular polythiophene thin film transistors, Adv. Funct. Mater. 15 (2005) 77–82.
[110] P. Checcoli, G. Conte, S. Salvatori, R. Paolesse, A. Bolognesi, M. Berliocchi, F. Brunetti, A. D'Amico, A. Di Carlo, P. Lugli, Tetra-phenyl porphyrin based thin film transistors, Synth. Met. 138 (2003) 261–266.
[111] M. Neghabi, A. Behjat, B.B. Fatemeh Mirjalili, L. Zamani, Improvement of performance of tetraphenylporphyrin-based red organic light emitting diodes using WO_3 and C_{60} buffer layers, Curr. Appl. Phys. 13 (2013) 302–306.
[112] X. Zhang, Q. Ma, K. Suzuki, A. Sugihara, G. Qin, T. Miyazaki, S. Mizukami, Magnetoresistance effect in rubrene-based spin valves at room temperature, ACS Appl. Mater. Interfaces 7 (2015) 4685–4692.
[113] J. Takeya, M. Yamagishi, Y. Tominari, R. Hirahara, Y. Nakazawa, T. Nishikawa, T. Kawase, T. Shimoda, S. Ogawa, Very high-mobility organic single-crystal transistors with in-crystal conduction channels, Appl. Phys. Lett. 90 (2007) 102120.
[114] H. Tatsuo, T. Jun, Organic field-effect transistors using single crystals, Sci. Tech. Adv. Mater. 10 (2009) 024314.
[115] S.Z. Bisri, T. Takenobu, T. Takahashi, Y. Iwasa, Electron transport in rubrene single-crystal transistors, Appl. Phys. Lett. 96 (2010) 183304.
[116] L. Wang, G. Lei, Y. Qiu, Bright white organic light-emitting diodes based on two blue emitters with similar molecular structures, J. Appl. Phys. 97 (2005) 114503.
[117] T. Ikegami, I. Kawayama, M. Tonouchi, S. Nakao, Y. Yamashita, H. Tada, Planar-type spin valves based on low-molecular-weight organic materials with $La_{0.67}Sr_{0.33}MnO_3$ electrodes, Appl. Phys. Lett. 92 (2008) 153304.
[118] S.W. Jiang, P. Wang, S.C. Jiang, B.B. Chen, M. Wang, Z.S. Jiang, D. Wu, Fabrication of lateral organic spin valves on $La_{0.7}Sr_{0.3}MnO_3$ electrodes, SPIN 04 (2014) 1440008.
[119] S. Lee, B. Koo, J. Shin, E. Lee, H. Park, H. Kim, Effects of hydroxyl groups in polymeric dielectrics on organic transistor performance, Appl. Phys. Lett. 88 (2006) 162109.
[120] J. Peng, Q. Sun, S. Wang, H.-Q. Wang, W. Ma, Low-temperature solution-processed alumina as gate dielectric for reducing the operating-voltage of organic field-effect transistors, Appl. Phys. Lett. 103 (2013) 061603.
[121] S. Yoo, B. Domercq, B. Kippelen, Efficient thin-film organic solar cells based on pentacene/C60 heterojunctions, Appl. Phys. Lett. 85 (2004) 5427–5429.
[122] Y. Kawasugi, T. Ujino, H. Tada, Room-temperature magnetoresistance in organic spin-valves based on a Co_2MnSi Heusler alloy, Org. Electron. 14 (2013) 3186–3189.
[123] L. Chen, G. Dong, L. Duan, L. Wang, J. Qiao, D. Zhang, Y. Qiu, Liquid-Formed Glassy Film of N,N′-Diphenyl-N,N′-bis(3-methylphenyl)benzidine: Formation, Carrier Transporting Ability, Photoluminescence, and Stability, J. Phys. Chem. C 111 (2007) 18376–18380.
[124] L. Zhu, H. Tang, Y. Harima, K. Yamashita, Y. Aso, T. Otsubo, Enhanced hole injection in organic light-emitting diodes consisting of self-assembled monolayer of tripod-shaped π-conjugated thiols, J. Mater. Chem. 12 (2002) 2250–2254.
[125] Y. Liu, T. Lee, H.E. Katz, D.H. Reich, Effects of carrier mobility and morphology in organic semiconductor spin valves, J. Appl. Phys. 105 (2009) 07C708.
[126] S.W. Jiang, P. Wang, B.B. Chen, Y. Zhou, H.F. Ding, D. Wu, Tuning carrier mobility without spin transport degrading in copper-phthalocyanine, Appl. Phys. Lett. 107 (2015) 042407.
[127] Y.R. Su, W.G. Xie, Y. Li, Y. Shi, N. Zhao, J.B. Xu, A low-temperature, solution-processed high- k dielectric for low-voltage, high-performance organic field-effect transistors (OFETs), J. Phys. D. Appl. Phys. 46 (2013) 095105.
[128] H. Vestweber, W. Rieß, Highly efficient and stable organic light-emitting diodes, Synth. Met. 91 (1997) 181–185.

[129] C. Hosokawa, H. Tokailin, H. Higashi, T. Kusumoto, Transient electroluminescence from hole transporting emitting layer in nanosecond region, Appl. Phys. Lett. 63 (1993) 1322–1324.
[130] N.H. Kim, Y.-H. Kim, J.-A. Yoon, S.Y. Lee, H.H. Yu, A. Turak, W.Y. Kim, High efficiency blue organic light emitting devices doped by BCzVBi in hole and electron transport layer, Mater. Res. Soc. Symp. Proc. 1567 (2013) 19–24.
[131] F. Li, T. Li, F. Chen, F. Zhang, Excellent spin transport in spin valves based on the conjugated polymer with high carrier mobility, Sci. Rep. 5 (2015) 9355.
[132] Z. Chen, Y. Zheng, H. Yan, A. Facchetti, Naphthalenedicarboximide- vs perylenedicarboximide-based copolymers. Synthesis and semiconducting properties in bottom-gate N-Channel organic transistors, J. Am. Chem. Soc. 131 (2009) 8–9.
[133] X. Sun, A. Bedoya-Pinto, R. Llopis, F. Casanova, L.E. Hueso, Flexible semi-transparent organic spin valve based on bathocuproine, Appl. Phys. Lett. 105 (2014) 083302.
[134] A.P. Kulkarni, C.J. Tonzola, A. Babel, S.A. Jenekhe, Electron transport materials for organic light-emitting diodes, Chem. Mater. 16 (2004) 4556–4573.
[135] J.S. Jiang, J.E. Pearson, S.D. Bader, Absence of spin transport in the organic semiconductor Alq_3, Phys. Rev. B 77 (2008) 035303.
[136] K. Ando, S. Watanabe, S. Mooser, E. Saitoh, H. Sirringhaus, Solution-processed organic spin–charge converter, Nat. Mater. 12 (2013) 622–627.
[137] S.W. Jiang, S. Liu, P. Wang, Z.Z. Luan, X.D. Tao, H.F. Ding, D. Wu, Exchange-dominated pure spin current transport in Alq_3 molecules, Phys. Rev. Lett. 115 (2015) 086601.
[138] D. Sun, K.J. van Schooten, M. Kavand, H. Malissa, C. Zhang, M. Groesbeck, C. Boehme, Z. Valy Vardeny, Inverse spin Hall effect from pulsed spin current in organic semiconductors with tunable spin-orbit coupling, Nat. Mater. 15 (2016) 863–869.
[139] M. Sayani, S.M. Himadri, L. Reino, Ö. Ronald, Organic spin valves: effect of magnetic impurities on the spin transport properties of polymer spacers, New J. Phys. 11 (2009) 013022.
[140] R. Lin, F. Wang, J. Rybicki, M. Wohlgenannt, K.A. Hutchinson, Distinguishing between tunneling and injection regimes of ferromagnet/organic semiconductor/ferromagnet junctions, Phys. Rev. B 81 (2010) 195214.
[141] J. Rybicki, R. Lin, F. Wang, M. Wohlgenannt, C. He, T. Sanders, Y. Suzuki, Tuning the performance of organic spintronic devices using X-ray generated traps, Phys. Rev. Lett. 109 (2012) 076603.
[142] B.B. Chen, S. Wang, S.W. Jiang, Z.G. Yu, X.G. Wan, H.F. Ding, D. Wu, The role of heavy metal ions on spin transport in organic semiconductors, New J. Phys. 17 (2015) 013004.
[143] S. Majumdar, H.S. Majumdar, On the origin of decay of spin current with temperature in organic spintronic devices, Org. Electron. 13 (2012) 2653–2658.
[144] B.-B. Chen, S.-W. Jiang, H.-F. Ding, Z.-S. Jiang, D. Wu, The basis of organic spintronics: fabrication of organic spin valves, Chin. Phys. B 23 (2014) 018104.
[145] T.D. Nguyen, G. Hukic-Markosian, F. Wang, L. Wojcik, X.-G. Li, E. Ehrenfreund, Z.V. Vardeny, The hyperfine interaction role in the spin response of π-conjugated polymer films and spin valve devices, Synth. Met. 161 (2011) 598–603.
[146] T.D. Nguyen, B.R. Gautam, E. Ehrenfreund, Z.V. Vardeny, Magnetoconductance response in unipolar and bipolar organic diodes at ultrasmall fields, Phys. Rev. Lett. 105 (2010) 166804.
[147] T.D. Nguyen, Y. Sheng, M. Wohlgenannt, T.D. Anthopoulos, On the role of hydrogen in organic magnetoresistance: a study of C60 devices, Synth. Met. 157 (2007) 930–934.
[148] T.D. Nguyen, Y. Sheng, J. Rybicki, G. Veeraraghavan, M. Wohlgenannt, Magnetoresistance in π-conjugated organic sandwich devices with varying hyperfine and spin-orbit coupling strengths, and varying dopant concentrations, J. Mater. Chem. 17 (2007) 1995–2001.
[149] B. Koopmans, Organic spintronics: pumping spins through polymers, Nat. Phys. 10 (2014) 249–250.
[150] M.A. Baldo, D.F. O'Brien, Y. You, A. Shoustikov, S. Sibley, M.E. Thompson, S.R. Forrest, Highly efficient phosphorescent emission from organic electroluminescent devices, Nature 395 (1998) 151–154.
[151] N.J. Rolfe, M. Heeney, P.B. Wyatt, A.J. Drew, T. Kreouzis, W.P. Gillin, Elucidating the role of hyperfine interactions on organic magnetoresistance using deuterated aluminium tris(8-hydroxyquinoline), Phys. Rev. B 80 (2009) 241201.
[152] Y. Sheng, T.D. Nguyen, G. Veeraraghavan, Ö. Mermer, M. Wohlgenannt, Effect of spin-orbit coupling on magnetoresistance in organic semiconductors, Phys. Rev. B 75 (2007) 035202.
[153] P. Shakya, P. Desai, M. Somerton, G. Gannaway, T. Kreouzis, W.P. Gillin, The magnetic field effect on the transport and efficiency of group III tris(8-hydroxyquinoline) organic light emitting diodes, J. Appl. Phys. 103 (2008) 103715.
[154] L. Nuccio, M. Willis, L. Schulz, S. Fratini, F. Messina, M. D'Amico, F.L. Pratt, J.S. Lord, I. McKenzie, M. Loth, B. Purushothaman, J. Anthony, M. Heeney, R.M. Wilson, I. Hernández, M. Cannas, K. Sedlak, T. Kreouzis, W.P. Gillin, C. Bernhard, A.J. Drew, Importance of spin-orbit interaction for the electron spin relaxation in organic semiconductors, Phys. Rev. Lett. 110 (2013) 216602.
[155] S. Liang, R. Geng, B. Yang, W. Zhao, R. Chandra Subedi, X. Li, X. Han, T.D. Nguyen, Curvature-enhanced spin-orbit coupling and spinterface effect in fullerene-based spin valves, Sci. Rep. 6 (2016) 19461.
[156] R. Lin, F. Wang, M. Wohlgenannt, C. He, X. Zhai, Y. Suzuki, Organic spin-valves based on fullerene C60, Synth. Met. 161 (2011) 553–557.
[157] X. Zhang, S. Mizukami, T. Kubota, Q. Ma, M. Oogane, H. Naganuma, Y. Ando, T. Miyazaki, Observation of a large spin-dependent transport length in organic spin valves at room temperature, Nat. Commun. 4 (2013) 1392.
[158] M. Gobbi, F. Golmar, R. Llopis, F. Casanova, L.E. Hueso, Room-temperature spin transport in C-60-Based spin valves, Adv. Mater. 23 (2011) 1609–1613.
[159] T.D. Nguyen, F. Wang, X.-G. Li, E. Ehrenfreund, Z.V. Vardeny, Spin diffusion in fullerene-based devices: morphology effect, Phys. Rev. B 87 (2013) 075205.
[160] Z.G. Yu, Suppression of the Hanle effect in organic spintronic devices, Phys. Rev. Lett. 111 (2013) 016601.
[161] Z.G. Yu, Spin-orbit coupling and its effects in organic solids, Phys. Rev. B 85 (2012) 115201.
[162] N.J. Harmon, M.E. Flatté, Distinguishing spin relaxation mechanisms in organic semiconductors, Phys. Rev. Lett. 110 (2013) 176602.
[163] J.-W. Yoo, H.W. Jang, V.N. Prigodin, C. Kao, C.B. Eom, A.J. Epstein, Giant magnetoresistance in ferromagnet/organic semiconductor/ferromagnet heterojunctions, Phys. Rev. B 80 (2009) 205207.
[164] S. Majumdar, H.S. Majumdar, Decay in spin diffusion length with temperature in organic semiconductors—An insight of possible mechanisms, Synth. Met. 173 (2013) 26–30.
[165] C. Boehme, J.M. Lupton, Challenges for organic spintronics, Nat. Nanotechnol. 8 (2013) 612–615.
[166] S. Sanvito, Molecular spintronics: the rise of spinterface science, Nat. Phys. 6 (2010) 562–564.
[167] K.V. Raman, A.M. Kamerbeek, A. Mukherjee, N. Atodiresei, T.K. Sen, P. Lazic, V. Caciuc, R. Michel, D. Stalke, S.K. Mandal, S. Blugel, M. Munzenberg, J.S. Moodera, Interface-engineered templates for molecular spin memory devices, Nature 493 (2013) 509–513.
[168] D. Çakır, D.M. Otálvaro, G. Brocks, From spin-polarized interfaces to giant magnetoresistance in organic spin valves, Phys. Rev. B 89 (2014) 115407.
[169] N. Baadji, S. Sanvito, Giant resistance change across the phase transition in spin-crossover molecules, Phys. Rev. Lett. 108 (2012) 217201.
[170] L. Schulz, L. Nuccio, M. Willis, P. Desai, P. Shakya, T. Kreouzis, V.K. Malik, C. Bernhard, F.L. Pratt, N.A. Morley, A. Suter, G.J. Nieuwenhuys, T. Prokscha, E. Morenzoni, W.P. Gillin, A.J. Drew, Engineering spin propagation across a hybrid organic/inorganic interface using a polar layer, Nat. Mater. 10 (2011) 39–44.
[171] K. Ihm, T.-H. Kang, K.-J. Kim, C.-C. Hwang, Y.-J. Park, K.-B. Lee, B. Kim, C.-H. Jeon, C.-Y. Park, K. Kim, Y.-H. Tak, Band bending of LiF/Alq_3 interface in organic light-emitting diodes, Appl. Phys. Lett. 83 (2003) 2949–2951.
[172] M.A. Baldo, S.R. Forrest, Interface-limited injection in amorphous organic semiconductors, Phys. Rev. B 64 (2001) 085201.
[173] F.A. Ma/'Mari, T. Moorsom, G. Teobaldi, W. Deacon, T. Prokscha, H. Luetkens, S. Lee, G.E. Sterbinsky, D.A. Arena, D.A. MacLaren, M. Flokstra, M. Ali, M.C. Wheeler, G. Burnell, B.J. Hickey, O. Cespedes, Beating the Stoner criterion using molecular interfaces, Nature 524 (2015) 69–73.
[174] R. Geng, A. Roy, W. Zhao, R.C. Subedi, X. Li, J. Locklin, T.D. Nguyen, Engineering of spin injection and spin transport in organic spin valves using π-conjugated polymer brushes, Adv. Funct. Mater. 26 (2016) 3999–4006.
[175] M. Grobosch, M. Knupfer, Electronic properties of organic semiconductor/electrode interfaces: the influence of contact contaminations on the interface energetic, Open Appl. Phys. J. 4 (2011) 8–18.
[176] Z.G. Yu, Impurity-band transport in organic spin valves, Nat. Commun. 5 (2014) 4842.
[177] F.J. Jedema, A.T. Filip, B.J. van Wees, Electrical spin injection and accumulation at room temperature in an all-metal mesoscopic spin valve, Nature 410 (2001) 345–348.
[178] M. Johnson, R.H. Silsbee, Interfacial charge-spin coupling: injection and detection of spin magnetization in metals, Phys. Rev. Lett. 55 (1985) 1790–1793.
[179] A. Riminucci, M. Prezioso, C. Pernechele, P. Graziosi, I. Bergenti, R. Cecchini, M. Calbucci, M. Solzi, V. Alek Dediu, Hanle effect missing in a prototypical organic spintronic device, Appl. Phys. Lett. 102 (2013) 092407.
[180] M. Grünewald, R. Göckeritz, N. Homonnay, F. Würthner, L.W. Molenkamp, G. Schmidt, Vertical organic spin valves in perpendicular magnetic fields, Phys. Rev. B 88 (2013) 085319.
[181] G. Salis, S.F. Alvarado, M. Tschudy, T. Brunschwiler, R. Allenspach, Hysteretic electroluminescence in organic light-emitting diodes for spin injection, Phys. Rev. B 70 (2004) 085203.
[182] T.D. Nguyen, E. Ehrenfreund, Z.V. Vardeny, Spin-polarized light-emitting diode based on an organic bipolar spin valve, Science 337 (2012) 204–209.
[183] S. Guenes, H. Neugebauer, N.S. Sariciftci, Conjugated polymer-based organic solar cells, Chem. Rev. 107 (2007) 1324–1338.
[184] F. Montaigne, J. Nassar, A. Vaurès, F.N. Van Dau, F. Petroff, A. Schuhl, A. Fert, Enhanced tunnel magnetoresistance at high bias voltage in double-barrier planar junctions, Appl. Phys. Lett. 73 (1998) 2829–2831.
[185] S.H. Liang, R. Geng, Q.T. Zhang, L. You, R.C. Subedi, J. Wang, X.F. Han, T.D. Nguyen, Large magnetoresistance at high bias voltage in double-layer organic spin valves, Org. Electron. 26 (2015) 314–318.
[186] V. Podzorov, E. Menard, A. Borissov, V. Kiryukhin, J.A. Rogers, M.E. Gershenson, Intrinsic charge transport on the surface of organic semiconductors, Phys. Rev. Lett. 93 (2004) 086602.

[187] V.C. Sundar, J. Zaumseil, V. Podzorov, E. Menard, R.L. Willett, T. Someya, M.E. Gershenson, J.A. Rogers, Elastomeric transistor stamps: reversible probing of charge transport in organic crystals, Science 303 (2004) 1644–1646.
[188] P. Prins, F.C. Grozema, J.M. Schins, T.J. Savenije, S. Patil, U. Scherf, L.D.A. Siebbeles, Effect of intermolecular disorder on the intrachain charge transport in ladder-type poly(*p*-phenylenes), Phys. Rev. B 73 (2006) 045204.
[189] B. Huang, D.J. Monsma, I. Appelbaum, Coherent spin transport through a 350 micron thick silicon wafer, Phys. Rev. Lett. 99 (2007) 177209.
[190] N. Tombros, C. Jozsa, M. Popinciuc, H.T. Jonkman, B.J. van Wees, Electronic spin transport and spin precession in single graphene layers at room temperature, Nature 448 (2007) 571–574.
[191] Z.G. Yu, Spin transport and the Hanle effect in organic spintronics, Nanoelectron. Spintron. 1 (2015), 2352–3951.